LIGO Laboratory / LIGO Scientific Collaboration

LIGO- T1100165-v2 *LIGO* 06/15/11

AOS SLC
Manifold/Cryopump and Mode Cleaner Tube Baffles FDR

Michael Smith, Heidy Kelman, Tim Nguyen, Virginio Sannibale, Lisa C. Austin

Distribution of this document:
LIGO Scientific Collaboration

This is an internal working note
of the LIGO Laboratory.

California Institute of Technology
LIGO Project – MS 18-34
1200 E. California Blvd.
Pasadena, CA 91125
Phone (626) 395-2129
Fax (626) 304-9834
E-mail: info@ligo.caltech.edu

Massachusetts Institute of Technology
LIGO Project – NW22-295
185 Albany St
Cambridge, MA 02139
Phone (617) 253-4824
Fax (617) 253-7014
E-mail: info@ligo.mit.edu

LIGO Hanford Observatory
P.O. Box 159
Richland WA 99352
Phone 509-372-8106
Fax 509-372-8137

LIGO Livingston Observatory
P.O. Box 940
Livingston, LA 70754
Phone 225-686-3100
Fax 225-686-7189

http://www.ligo.caltech.edu/

Table of Contents

1 INTRODUCTION *6*

1.1 Final Design Review Checklist **6**
1.1.1 Final requirements – any changes or refinements from PDR? 6
Direct Requirements 6
Mode Cleaner Tube Baffle Requirements—NEW 6
Manifold/Cryopump Baffle Requirements 6
Clear Aperture Requirements 6
1.1.2 Resolutions of action items from SLC PDR 6
Lower BRDF Material for Baffles 6
Viton O-Ring Suspension 6
Earthquake Stops 7
1.1.3 Subsystem block and functional diagrams 7
1.1.4 Final Parts Lists and Drawing Package 7
1.1.5 Final specifications 7
1.1.6 Final interface control documents 7
1.1.7 Relevant RODA changes and actions completed 7
1.1.8 Signed Hazard Analysis 7
1.1.9 Final Failure Modes and Effects Analysis 7
1.1.10 Risk Registry items discussed 8
1.1.11 Design analysis and engineering test data 8
1.1.12 Software detailed design 8
1.1.13 Final approach to safety and use issues 8
1.1.14 Production Plans for Acquisition of Parts, Components, Materials Needed For Fabrication 8
1.1.15 Installation Plans and Procedures 8
1.1.16 Final hardware test plans 8
1.1.17 Final software test plans 8
1.1.18 Cost compatibility with cost book 8
1.1.19 Fabrication, installation and test schedule 9
1.1.20 Lessons Learned Documented, Circulated 9
1.1.20.1 Porcelainizing 9
1.1.21 Problems and concerns 9

1.2 Applicable Documents **9**

2 MODE CLEANER TUBE BAFFLE *10*

2.1 MODE CLEANER TUBE BAFFLE DESCRIPTION **10**

2.2 MODECLEANER TUBE BAFFLE LOCATIONS **10**
2.2.1 H1 and L1 10
2.2.2 H2 13

2.3 Detail of the Mode Cleaner Tube Baffles **15**
2.3.1 H1 Mode Cleaner Tube Baffles 15
2.3.2 L1 Mode Cleaner Tube Baffles 22
2.3.3 H2 Mode Cleaner Tube Baffles 23

2.4 Errant Beam Damage of the Mode Cleaner Tube Baffle 30
2.4.1 Loss of Lock of Power Recycling Cavity 30
2.4.2 Loss of Lock of Input Mode Cleaner Cavity 33
2.4.3 Continuous PSL Errant Beam Power 34
2.5 Errant Beam Damage of the Mode Cleaner Tube Baffle 34
2.6 Mechanical Interfaces 34
2.7 Optical Interfaces 34
2.7.1 Main IFO Beams 34
2.7.2 Optical Lever Beams 36
2.7.3 Video Camera Beams 36
3 MANIFOLD/CRYOPUMP BAFFLE 36
3.1 Manifold/Cryopump Baffle Characteristics 41
3.2 Manifold/Cryopump Baffle Suspension 41
3.2.1 Motion Transfer Function 43
3.2.2 Cryopump Baffle Surface BRDF 44
3.2.3 Cryopump Baffle Scatter 44
3.3 Optical Interface 46
4 INTERFACE CONTROL DOCUMENT 49

Table of Figures

Figure 1: MCA1 AND MCB1 11
Figure 2: MCA2 AND MCB2 12
Figure 3: MCA3 AND MCB3 13
Figure 4: MCA4 AND MCB4 14
Figure 5: Front View of MCA1 Mode Cleaner Tube Baffle 15
Figure 6: Back View of MCA1 Mode Cleaner Tube Baffle 16
Figure 7: Front View of MCB1 Mode Cleaner Tube Baffle 17
Figure 8: Back View of MCB1 Mode Cleaner Tube Baffle 18
Figure 9: Front View of MCA2 Mode Cleaner Tube Baffle 19
Figure 10: Back View of MCA2 Mode Cleaner Tube Baffle 20
Figure 11: Front View of MCB2 Mode Cleaner Tube Baffle 21
Figure 12: Back View of MCB2 Mode Cleaner Tube Baffle 22
Figure 13: Front View of MCA3 Mode Cleaner Tube Baffle 23
Figure 14: Back View of MCA3 Mode Cleaner Tube Baffle 24
Figure 15: Front View of MCB3 Mode Cleaner Tube Baffle 25
Figure 16: Back View of MCB3 Mode Cleaner Tube Baffle 26
Figure 17: Front View of MCA4 Mode Cleaner Tube Baffle 27
Figure 18: Back View of MCA4 Mode Cleaner Tube Baffle 28
Figure 19: Front View of MCB4 Mode Cleaner Tube Baffle 29
Figure 20: Back View of MCB4 Mode Cleaner Tube Baffle 30
Figure 21: Manifold/Cryopump Baffle Positioned in the Manifold Tube near A-1 Viewport Adapter 37
Figure 22: Manifold/Cryopump Baffle as Seen from the Near Test Mass 38

Figure 23: Manifold/Cryopump Baffle as Seen from the Cryopump and the Arm Beam Tube Direction *39*
Figure 24: 1st Article Manifold/Cryopump Baffle Suspended from the Balancing/Installation Fixture *40*
Figure 25: Close up of Blade Spring and 2-Wire Pendulum Suspension Mechanism *42*
Figure 26: Eddy-current Damping Mechanism *42*
Figure 27: Vertical Transfer Function of Suspended Manifold/Cryopump Baffle *43*
Figure 28: Axial Transfer Function of Suspended Manifold/Cryopump Baffle *44*
Figure 29: Cryopump Baffle Scattered Light Displacement Noise *46*
Figure 30: Clearance of Arm Cavity Beams through ITM Manifold/Cryopump Baffle *47*
Figure 31: Manifold/cryopump Baffle Fractional Power Absorption vs Horizontal De-centering Error *49*

1 INTRODUCTION

1.1 Final Design Review Checklist

1.1.1 Final requirements – any changes or refinements from PDR?

The requirements for the Manifold/Cryopump Baffle and the Mode Cleaner Tube Baffles are listed in T070061 Stray Light Control Design Requirements.

Direct Requirements

Phase noise due to scattered light fields injected into the interferometer is treated as a technical noise source. Therefore, the total scattered light phase noise, expressed in equivalent displacement noise, must be < $1/10^{th}$ of the quadrature sum of the suspension thermal noise and the test mass thermal noise (referred to as the SRD), as given in Figure 1 of M060056-06, Advanced LIGO Reference Design.

Mode Cleaner Tube Baffle Requirements—NEW

The Mode Cleaner Tube Baffles shall shield the corners of the mode cleaner tubes where they join the flat surface of the viewport adapters.

The Mode Cleaner Tube Baffles, near HAM2 and HAM8, shall help protect the triple mirror suspensions from damage by errant beams caused by loss of lock of the recycling cavity.

Manifold/Cryopump Baffle Requirements

The Manifold/Cryopump Baffles shall block scattered light from the HR surfaces of the ITM and ETM from impinging on the surfaces of the cryopumps in the arm cavity. They shall fit within the same space allocated to the Cryopump Baffles for Initial LIGO.

Clear Aperture Requirements

Shall not vignette the recycling cavity beam > 100 ppm power loss;

Shall not vignette the arm cavity beam > 1 ppm;

Shall not vignette the recycling cavity beams > 1 ppm;

Vignetting of the main beam by the cryopump baffles shall not significantly increase the power loss in the arm cavity

1.1.2 Resolutions of action items from SLC PDR

Refer to: LIGO-L0900119-v1

Lower BRDF Material for Baffles
We suggest the team consider a lower-BRDF material for the more critical baffles,
and in particular suggest looking at the electro-static frit black-enameled steel as an option
that would give better optical performance.
Ans: *We will use black porcelain applied to steel baffles using an electrostatic powder application process; See* ***Error! Reference source not found.****.*

Viton O-Ring Suspension
Review the tests that have been carried out with the Viton o-ring suspension (is there a

report available?).
Ans: *The o-ring suspension has been replaced with a maraging steel blade spring that suspends the manifold/cryopump baffle from a flexible wire. The baffle is damped with eddy-current damping magnets moving against a fixed copper plate mounted to the outer support ring.*

Earthquake Stops
Tell us more about how the EQ stops are to be mounted to the chamber.

Not applicable

1.1.3 Subsystem block and functional diagrams

Not applicable

1.1.4 Final Parts Lists and Drawing Package

E1000831-v1 BOM - aLIGO Mode Cleaner Tube Baffle Top Assembly

E1100422-v1 BOM - aLIGO Manifold Cryopump Tube Baffle Assembly

E1000360-v2 DCN - ALIGO Manifold-Cryo Baffle Assembly

E1000822-v1 DCN - ALIGO Mode Cleaner Tube Baffle

1.1.5 Final specifications

E1000083-v5 Specification for Enameled Steel to be used in the LIGO Ultra-High Vacuum System

E0900023-v11 PROCESS FOR MANUFACTURING CANTILEVER SPRING BLADES FOR AdvLIGO

E0900364-v8 Metal components intended for use in the Adv LIGO Vacuum System

1.1.6 Final interface control documents

The mechanical and optical interfaces of the Manifold/cryopump Baffle and the Mode Cleaner Tube Baffles are described in E1100583 SLC Manifold/Cryopump Baffle Interface Control Document.

1.1.7 Relevant RODA changes and actions completed

Not applicable

1.1.8 Signed Hazard Analysis

E1100482-v1 SLC Manifold/Cryopump Baffle Install Hazard Analysis

E1100491-v1 SLC Mode Cleaner Tube Baffle Install Hazard Analysis

1.1.9 Final Failure Modes and Effects Analysis

Not Required

1.1.10 Risk Registry items discussed

None for this subsystem

1.1.11 Design analysis and engineering test data

See **Error! Reference source not found.** and **Error! Reference source not found.**.

1.1.12 Software detailed design

Not applicable

1.1.13 Final approach to safety and use issues

No operational safety issues

1.1.14 Production Plans for Acquisition of Parts, Components, Materials Needed For Fabrication

E1100483 Manifold/Cryopump Baffle and Mode Cleaner Tube Baffle Production Plan

1.1.15 Installation Plans and Procedures

This will be deferred until after FDR

1.1.16 Final hardware test plans

- Tests of porcelainized witness samples: ball drop test, visual inspection

Witness samples taken during each furnace run for porcelainizing the baffle parts will be subjected to a visual inspection and to a standard ball drop test to determine if the adhesion of the porcelain material is sufficient.

- FTIR tests of porcelainized parts

A representative selection of porcelainized baffle parts from each furnace run will be swabbed and a proper FTIR sample collected for subsequent contamination evaluation.

- Blade stiffness measurement

See E1100481 Fabrication, Installation, and Test Plan

- Suspended baffle balancing before installation

See E1100481 Fabrication, Installation, and Test Plan

1.1.17 Final software test plans

Not applicable, ISC will handle this.

1.1.18 Cost compatibility with cost book

See E1100483 Manifold/Cryopump Baffle and Mode Cleaner Tube Baffle Production Plan

1.1.19 Fabrication, installation and test schedule

See E1100481-v1 Fabrication, Installation, and Test Plan

1.1.20 Lessons Learned Documented, Circulated

1.1.20.1 Porcelainizing

In order to maintain the flatness and avoid warping of flat porcelainized parts during the baking process in the continuous feed furnace, the parts must be suspended in such a way that the forces of gravity act in the plane of the part.

Fabricated non-planar shapes that have structural integrity are best porcelainized by using a stationary furnace, and placing the pieces so that gravity forces act normal to a plane of symmetry.

The first article manifold/cryopump baffle was coated with porcelain enamel using the wet slurry application process. In the future, the coating will be applied using an electrostatic powder application process. Preliminary measurements of the electrostatic power process indicate a factor 2 lower BRDF than with the wet slurry process. The electrostatic process cannot be used for coating parts that have narrow internal angles, such as the inside angles of the “W-shaped” center section of the ACB.

1.1.21 Problems and concerns

The Manifold/Cryopump baffle indicated numerous internal resonances of the baffle structure at frequencies above 100 Hz; however, the apparent displacement noise associated with those resonances appears to fall below the AOS requirement and are acceptable without any further stiffening of the baffle structure.

1.2 Applicable Documents

E0900023-v11_Manufacturing Process Spec for Cantilever Spring Blades

E0900364-v8 LIGO Metal in Vacuum

E1000083-v5_Spec for Enameled Steel Sheet

E1100481 Fabrication, Installation, and Test Plan

T060073-00 Transfer Functions of Injected Noise

T070061-v2 Stray light Control Design Requirements

T0900269-v2 Stray Light Control (SLC) Preliminary Design

T1100056-v2 Arm Cavity Baffle Edge Scatter

E1100482-v1 Manifold/Cryopump Baffle Install Hazard Analysis

E1100491-v1 Mode Cleaner Tube Baffle Install Hazard Analysis

E1100483-v1 Manifold/Cryopump Baffle and Mode Cleaner Tube Baffle Production Plan

2 MODE CLEANER TUBE BAFFLE

The mode cleaner tube baffles were added as a revision to the SLC Preliminary Design (T0900269-v2 Stray Light Control (SLC) Preliminary Design). It was discovered during the commissioning of eLIGO that apparent scattered light displacement noise occurred whenever light from the arm cavity or power recycling cavity was allowed to hit the frontal surface of viewport adapters or spool adapters at the junction of a larger diameter manifold tube or spool piece, e.g. the A-1 adapter connecting to the ITM B-9 spool, or the diameter transition where the signal recycling mode cleaner tube joins to HAM4 and HAM 5.

An additional function of the mode cleaner tube baffles, next to HAM2 and HAM8, is to help contain the errant beams that might hit the mirror structures on those chambers during inadvertent loss of lock of the power recycling cavity.

2.1 MODE CLEANER TUBE BAFFLE DESCRIPTION

All Mode Cleaner Tube Baffles are attached to a two-piece expansion ring that expands and presses against the inside of the mode cleaner tube.

An aluminum spoke structure serves as a mounting frame for the outer annular portion of the baffle, which is made from porcelainized steel with a relatively low BRDF of <0.05 sr^-1. The baffle is tilted at 5 deg to avoid any glints back toward the incident beam. The outer annular baffle section is brought into the tube in two pieces and is assembled and attached to the support ring. The holes in the outer annular baffle provide clear apertures for the viewports.

The inner portion of the baffle is made either from aluminum (e.g. MCA1 and MCA3), or porcelainized steel. It is also brought into the mode cleaner tube in two pieces and attached to the outer spoke structure. It has individual beam holes, or a larger single opening, to allow the various IFO beams, video camera beams, and optical lever beams to pass through the baffle. The aluminum versions do not require a spoke structure to support the inner baffle; however, the porcelainized steel versions have an inner spoke structure.

2.2 MODECLEANER TUBE BAFFLE LOCATIONS

2.2.1 H1 and L1

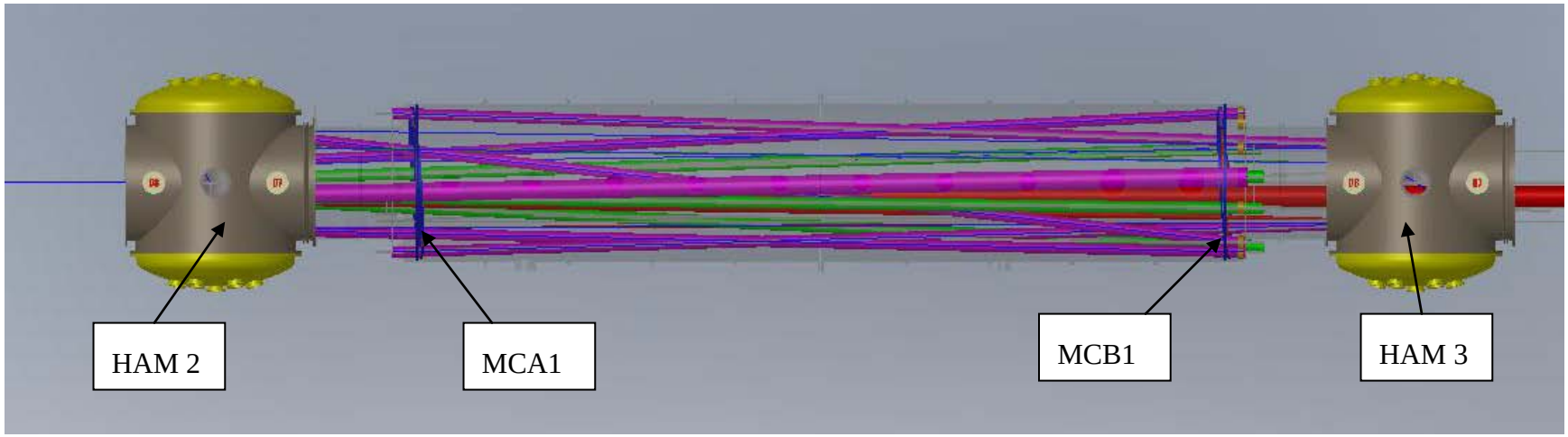

Figure 1: MCA1 AND MCB1

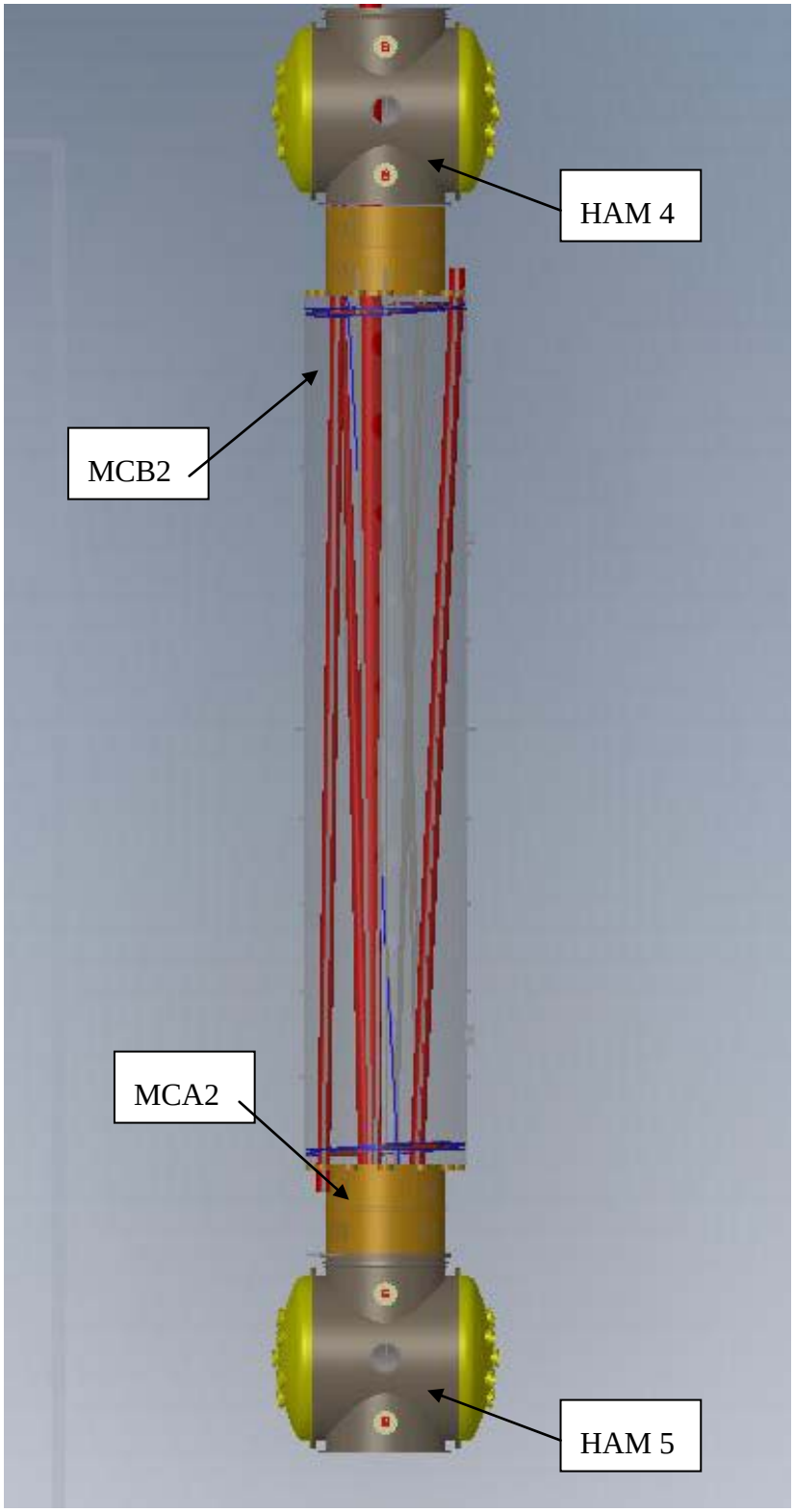

Figure 2: MCA2 AND MCB2

2.2.2 H2

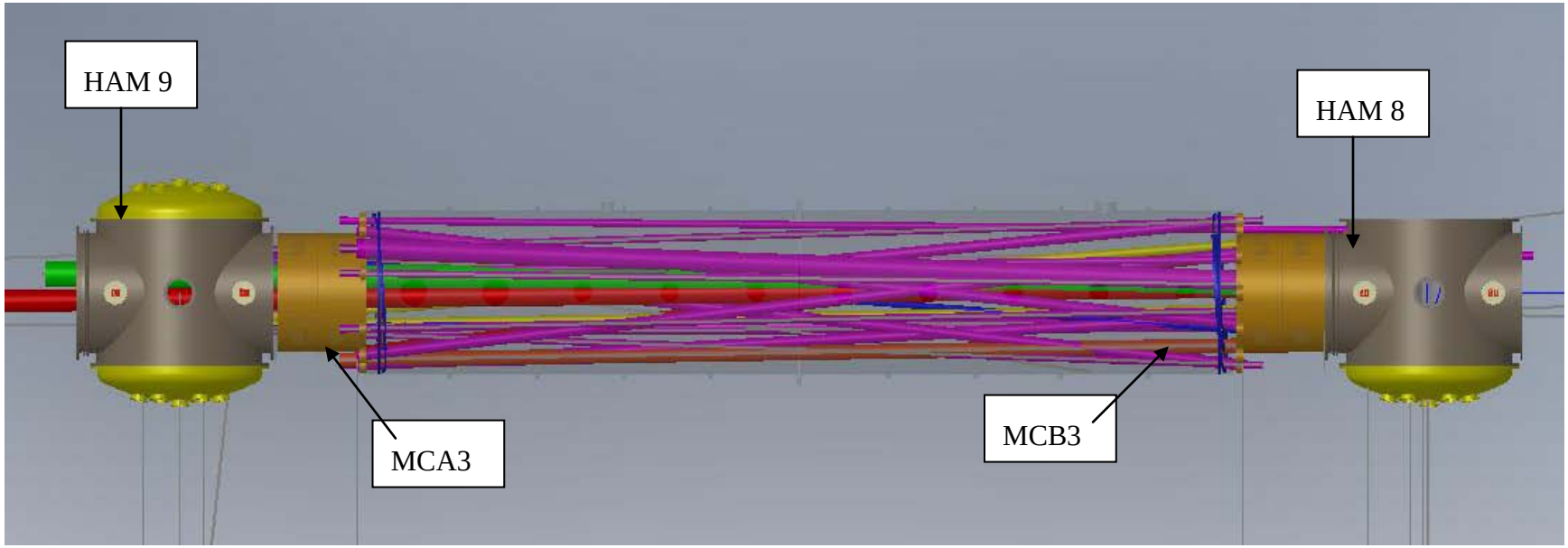

Figure 3: MCA3 AND MCB3

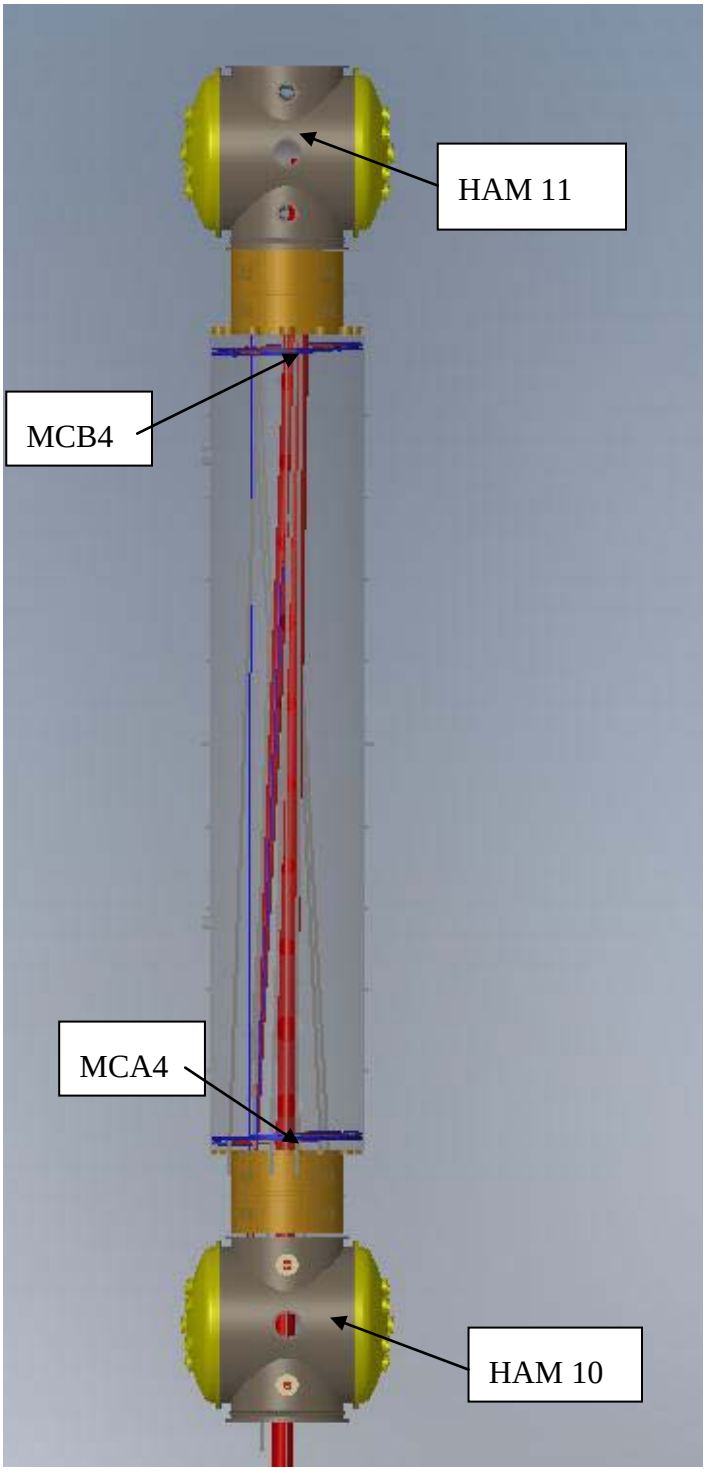

Figure 4: MCA4 AND MCB4

2.3 Detail of the Mode Cleaner Tube Baffles

The front view faces toward the inside of the mode cleaner tube. The back view faces toward the HAM chamber.

2.3.1 H1 Mode Cleaner Tube Baffles

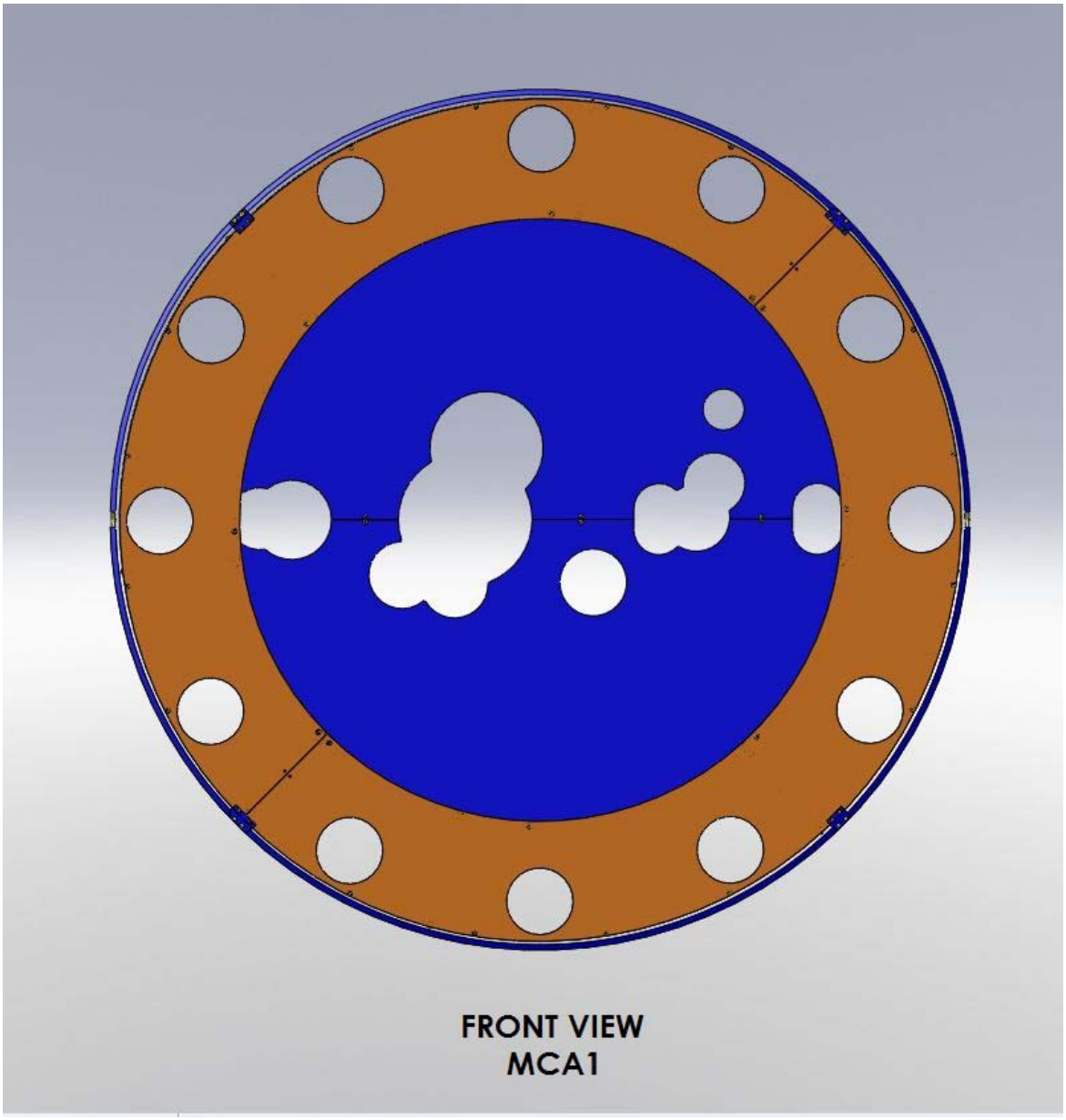

Figure 5: Front View of MCA1 Mode Cleaner Tube Baffle

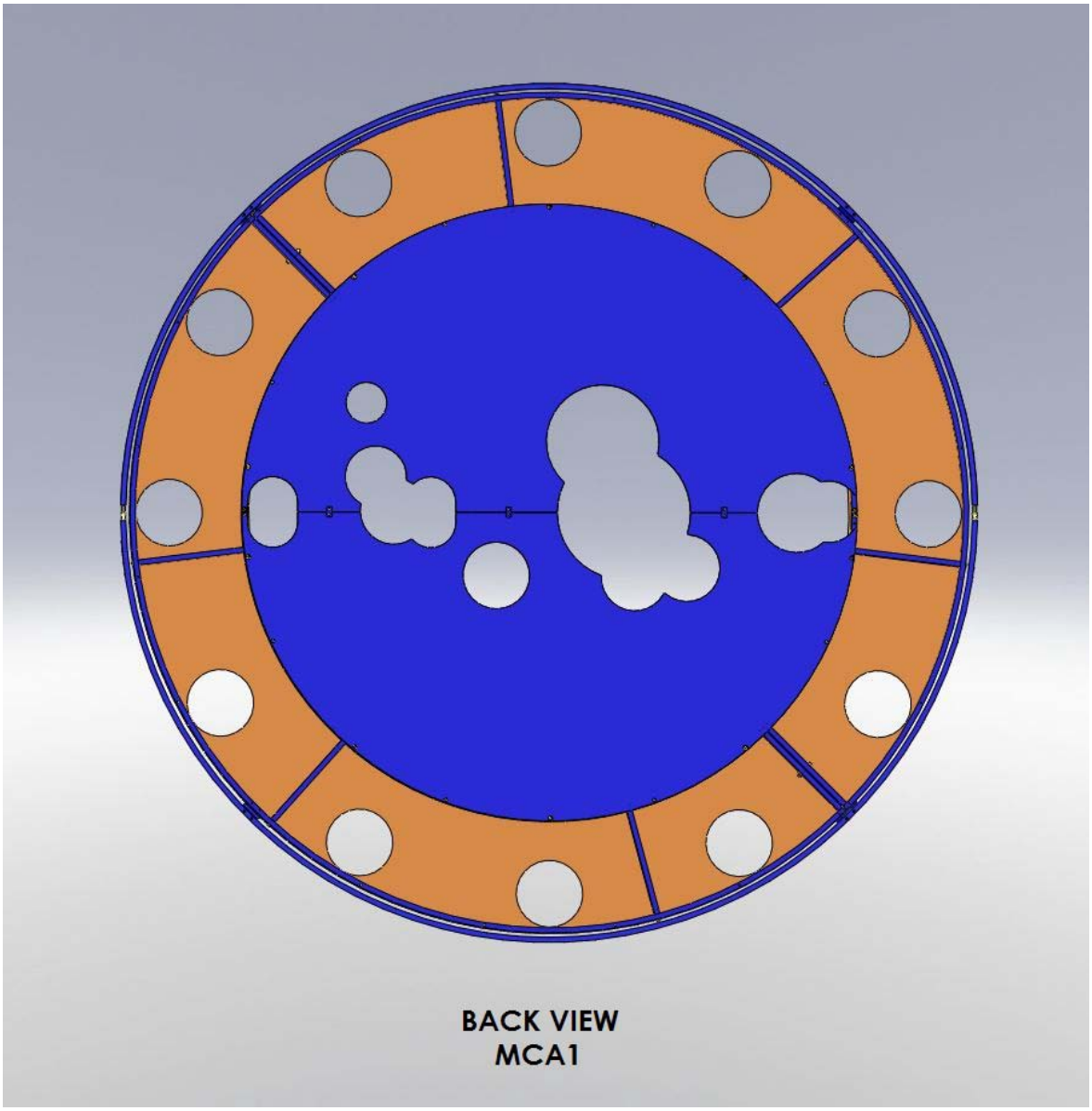

Figure 6: Back View of MCA1 Mode Cleaner Tube Baffle

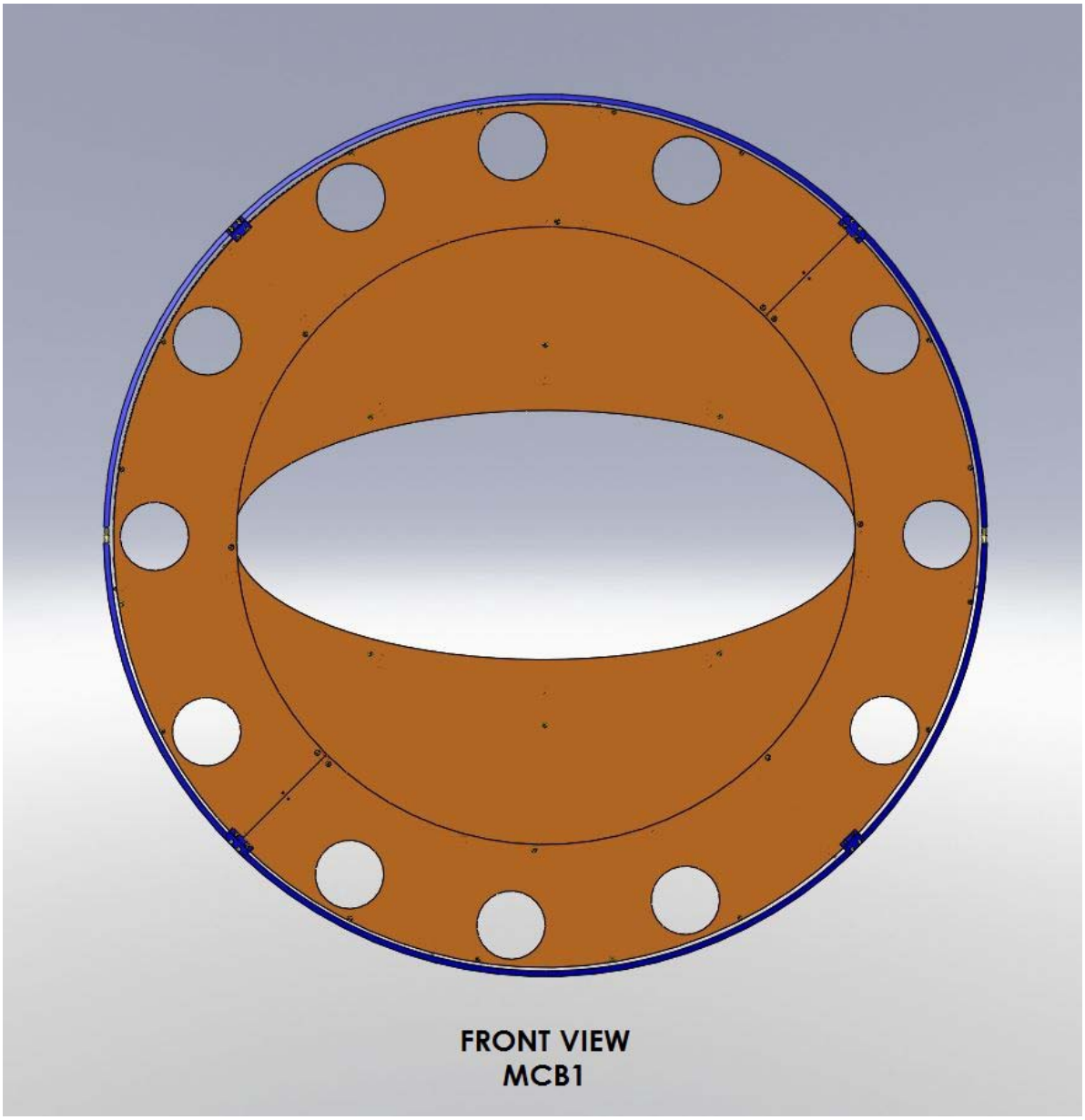

Figure 7: Front View of MCB1 Mode Cleaner Tube Baffle

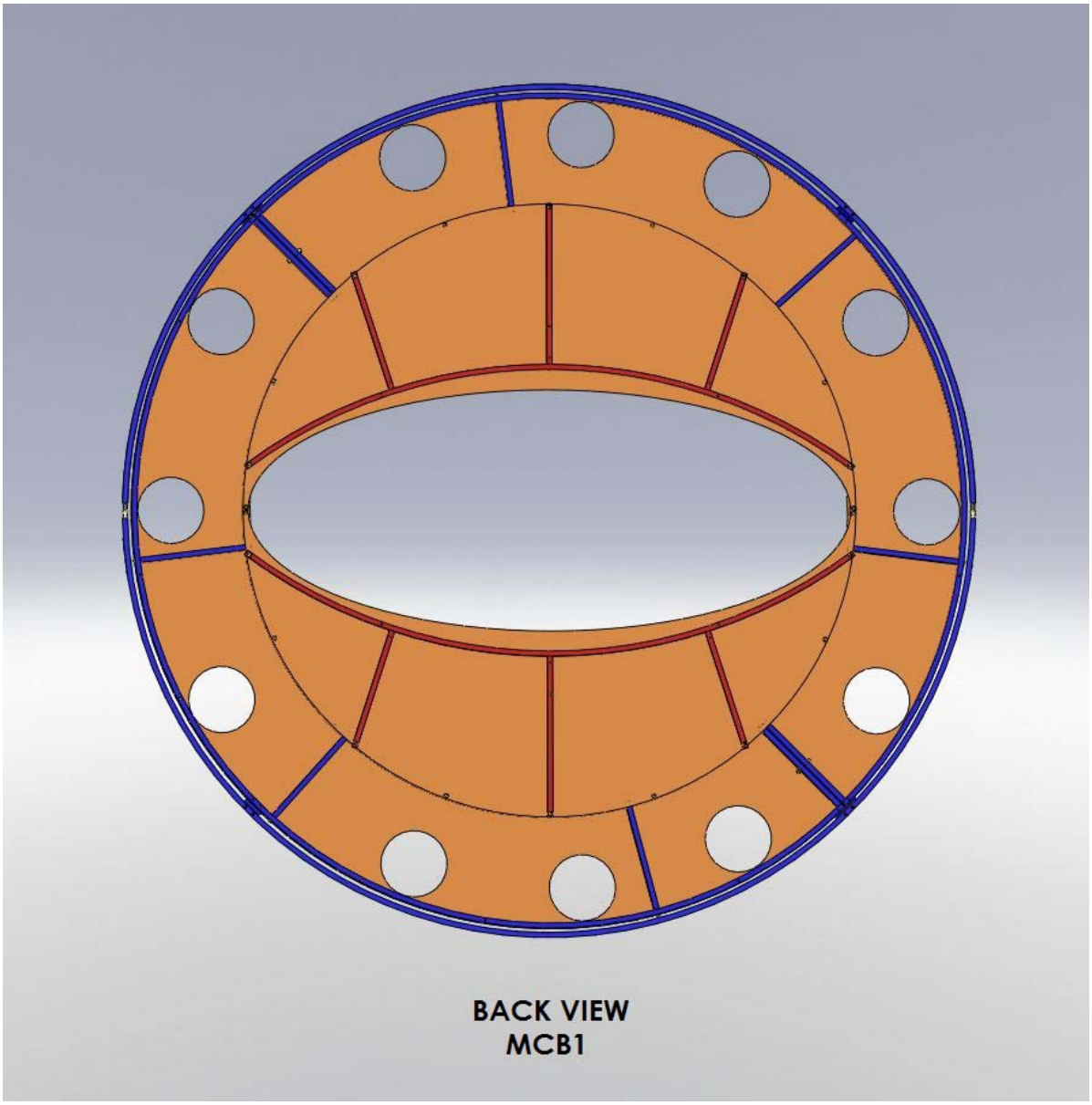

Figure 8: Back View of MCB1 Mode Cleaner Tube Baffle

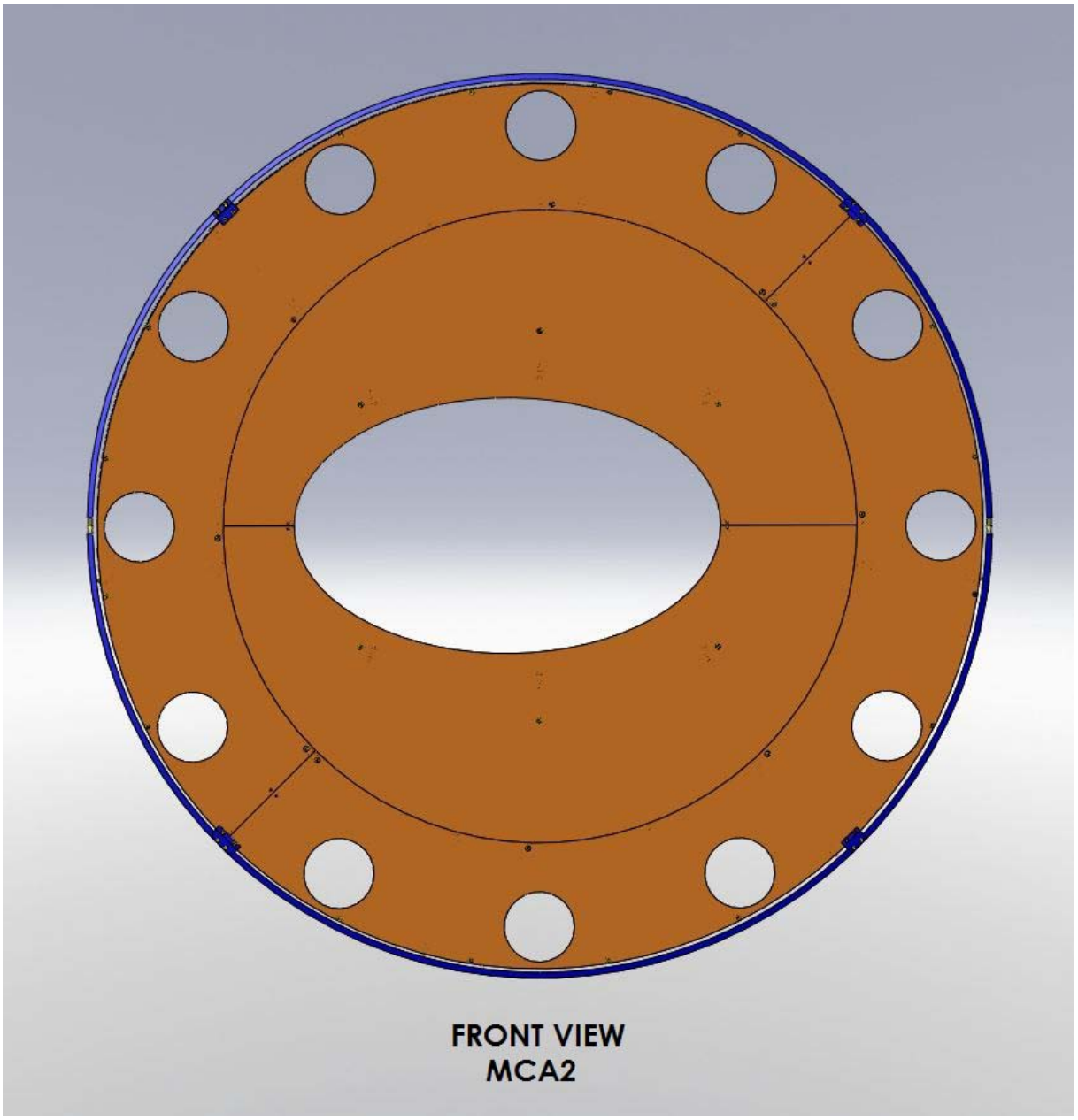

Figure 9: Front View of MCA2 Mode Cleaner Tube Baffle

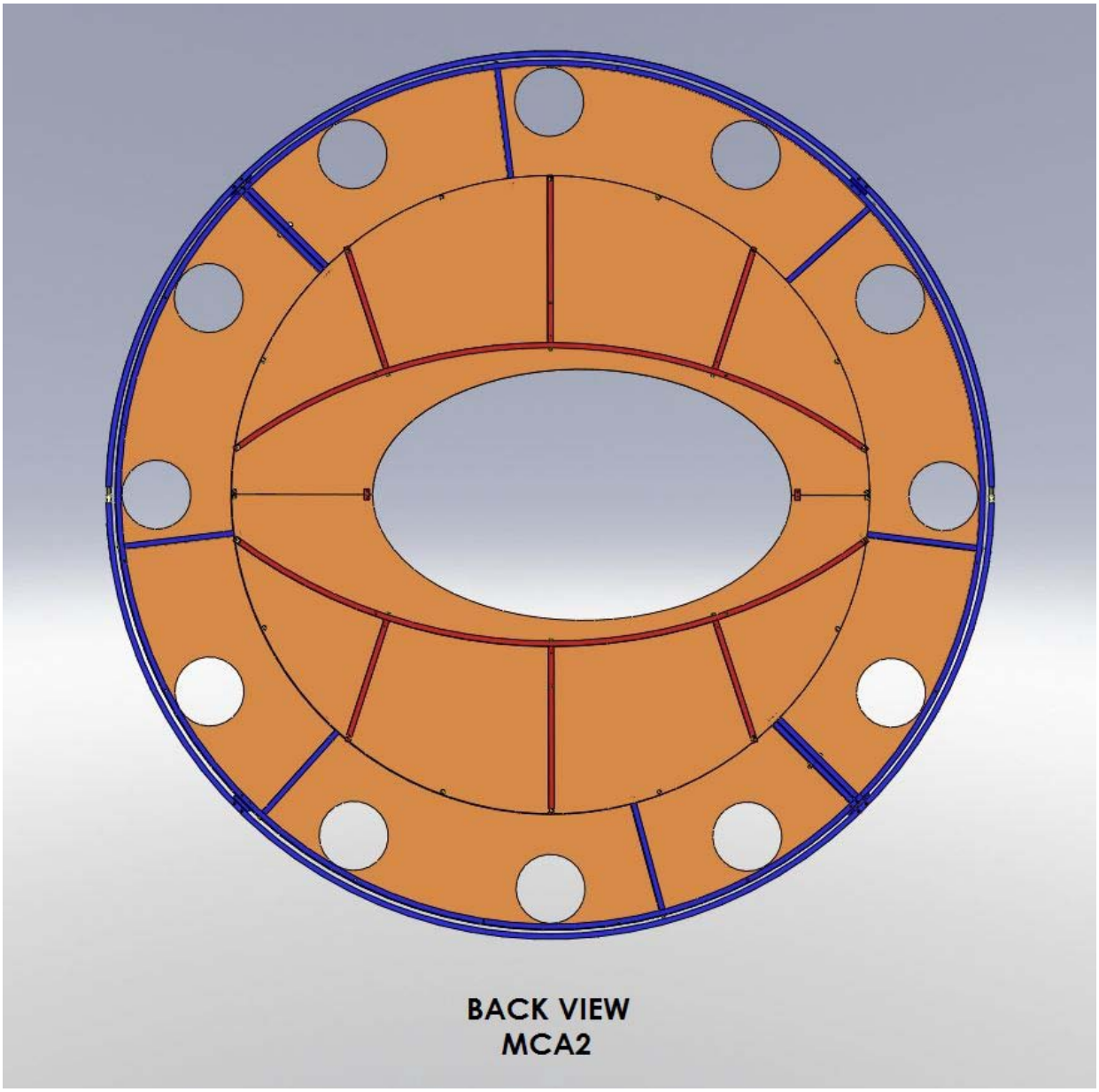

Figure 10: Back View of MCA2 Mode Cleaner Tube Baffle

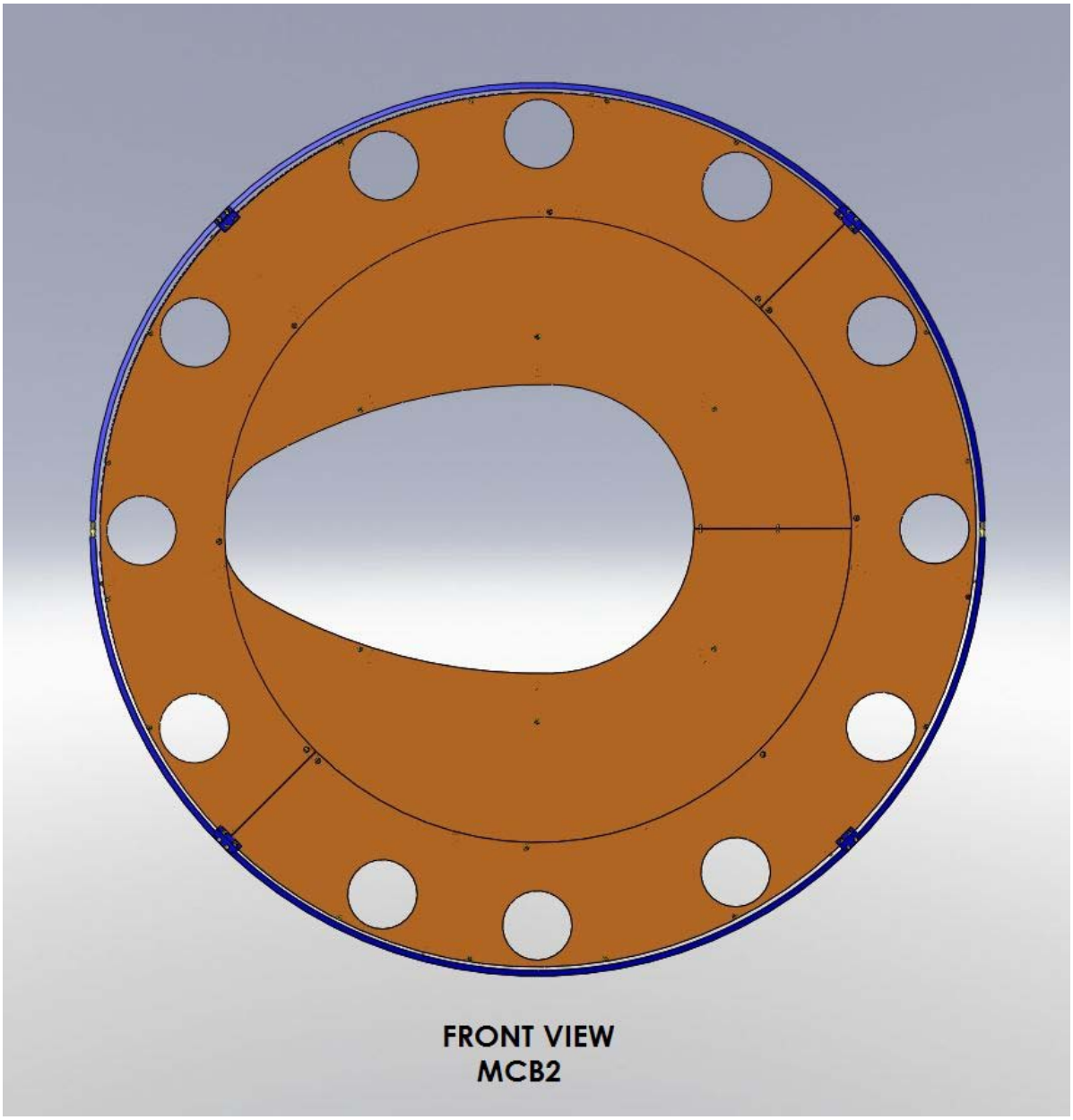

Figure 11: Front View of MCB2 Mode Cleaner Tube Baffle

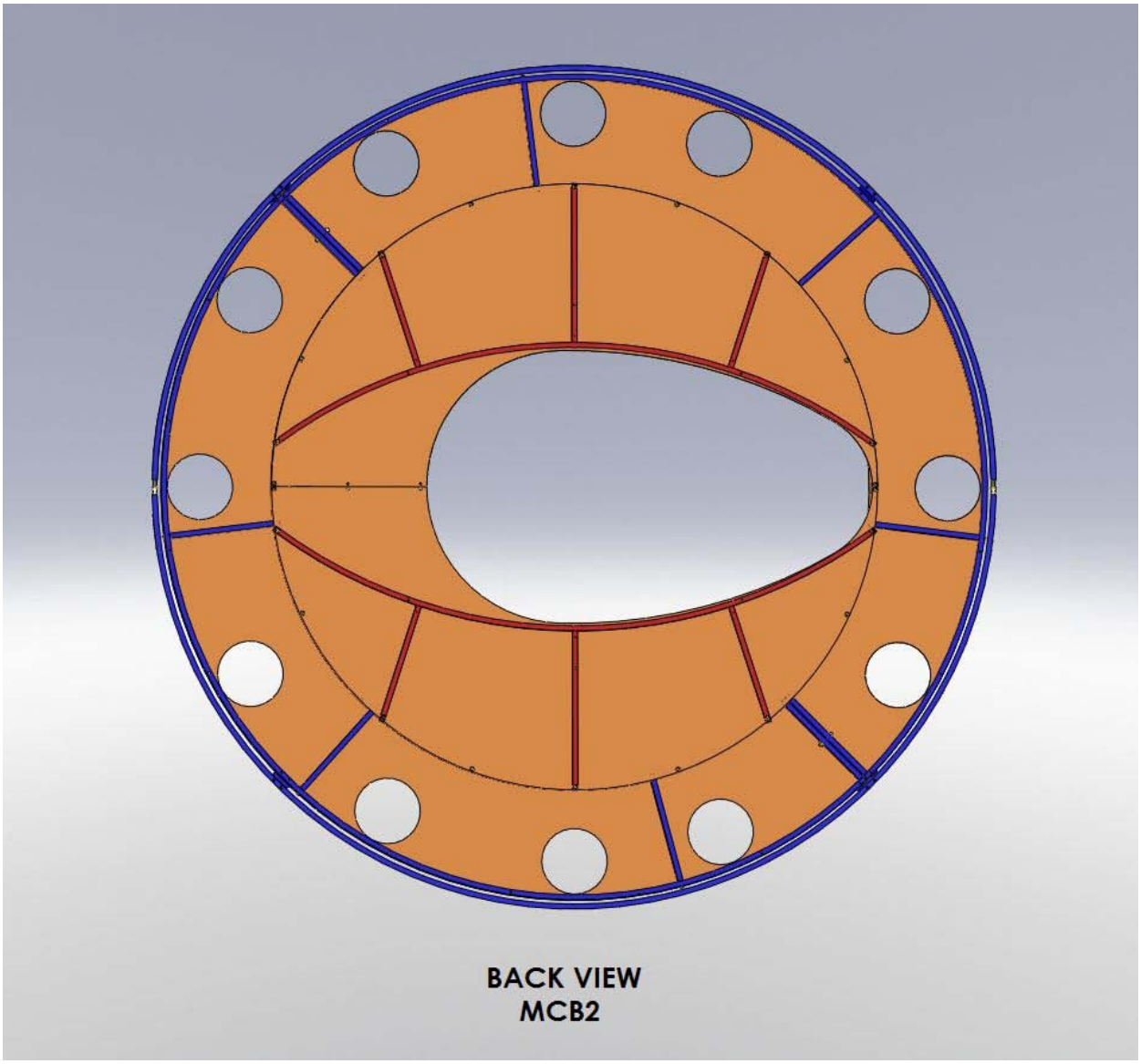

Figure 12: Back View of MCB2 Mode Cleaner Tube Baffle

2.3.2 L1 Mode Cleaner Tube Baffles

The L1 mode cleaner tube baffles are identical to the H1 baffles.

2.3.3 H2 Mode Cleaner Tube Baffles

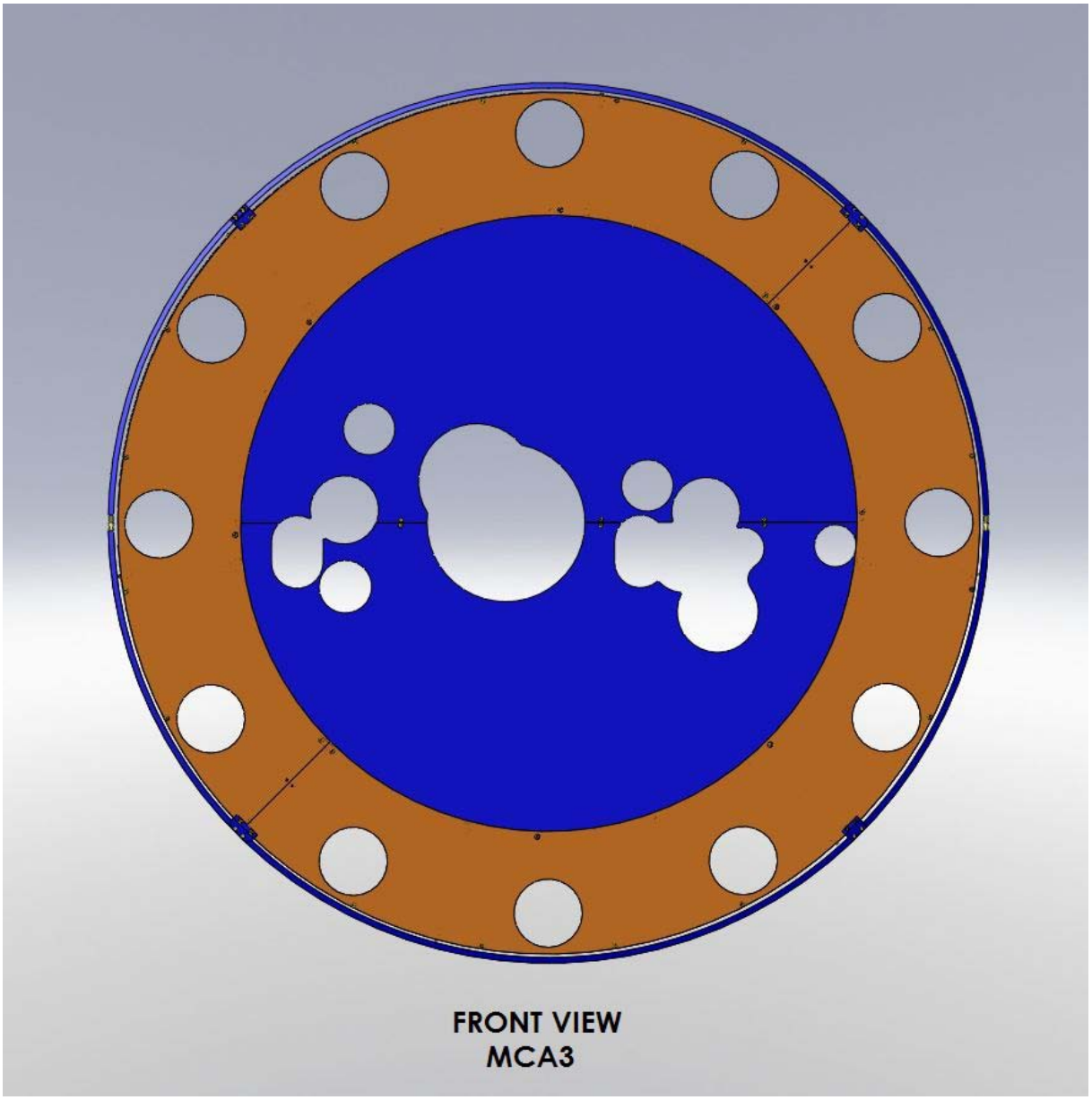

Figure 13: Front View of MCA3 Mode Cleaner Tube Baffle

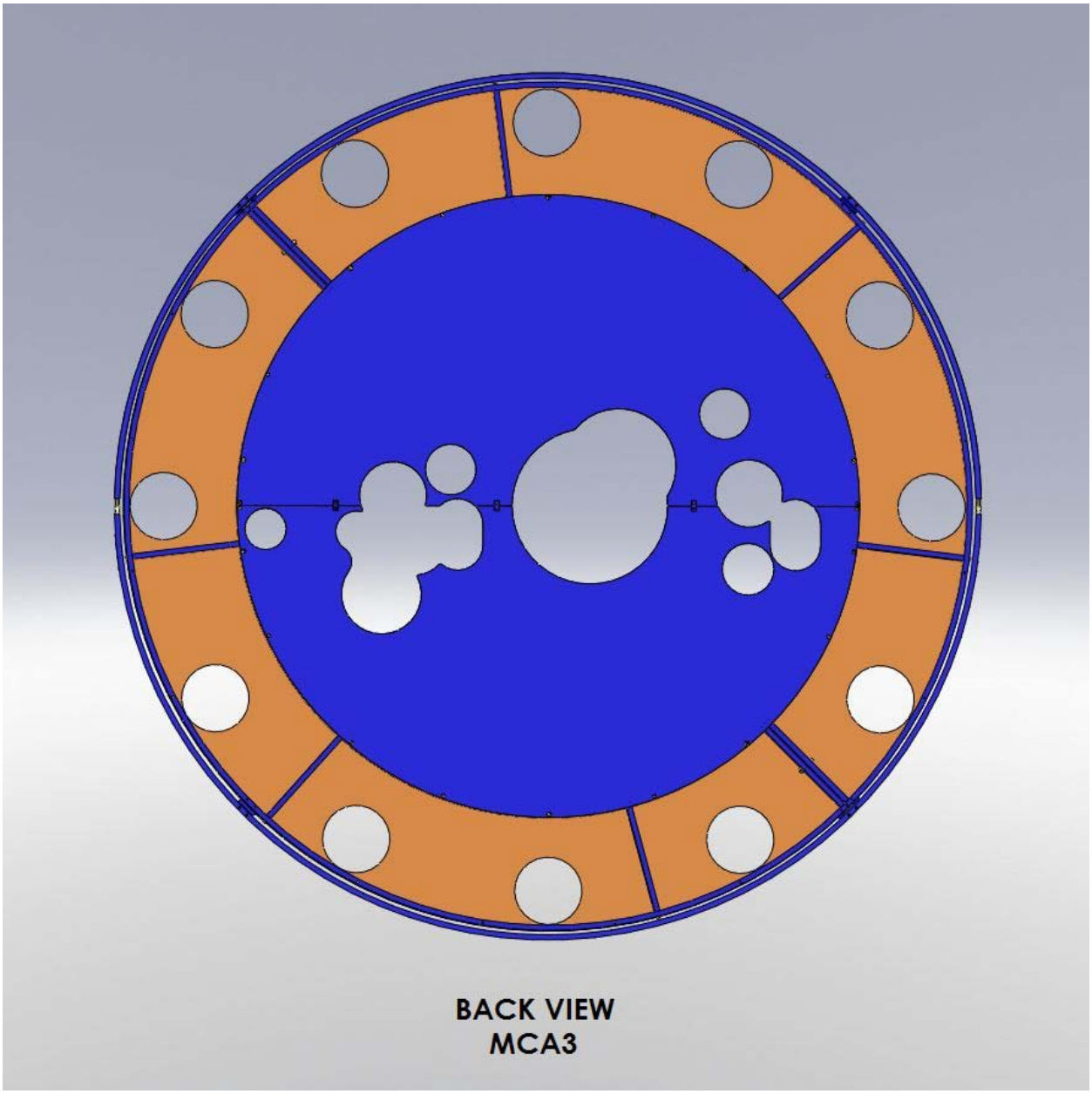

Figure 14: Back View of MCA3 Mode Cleaner Tube Baffle

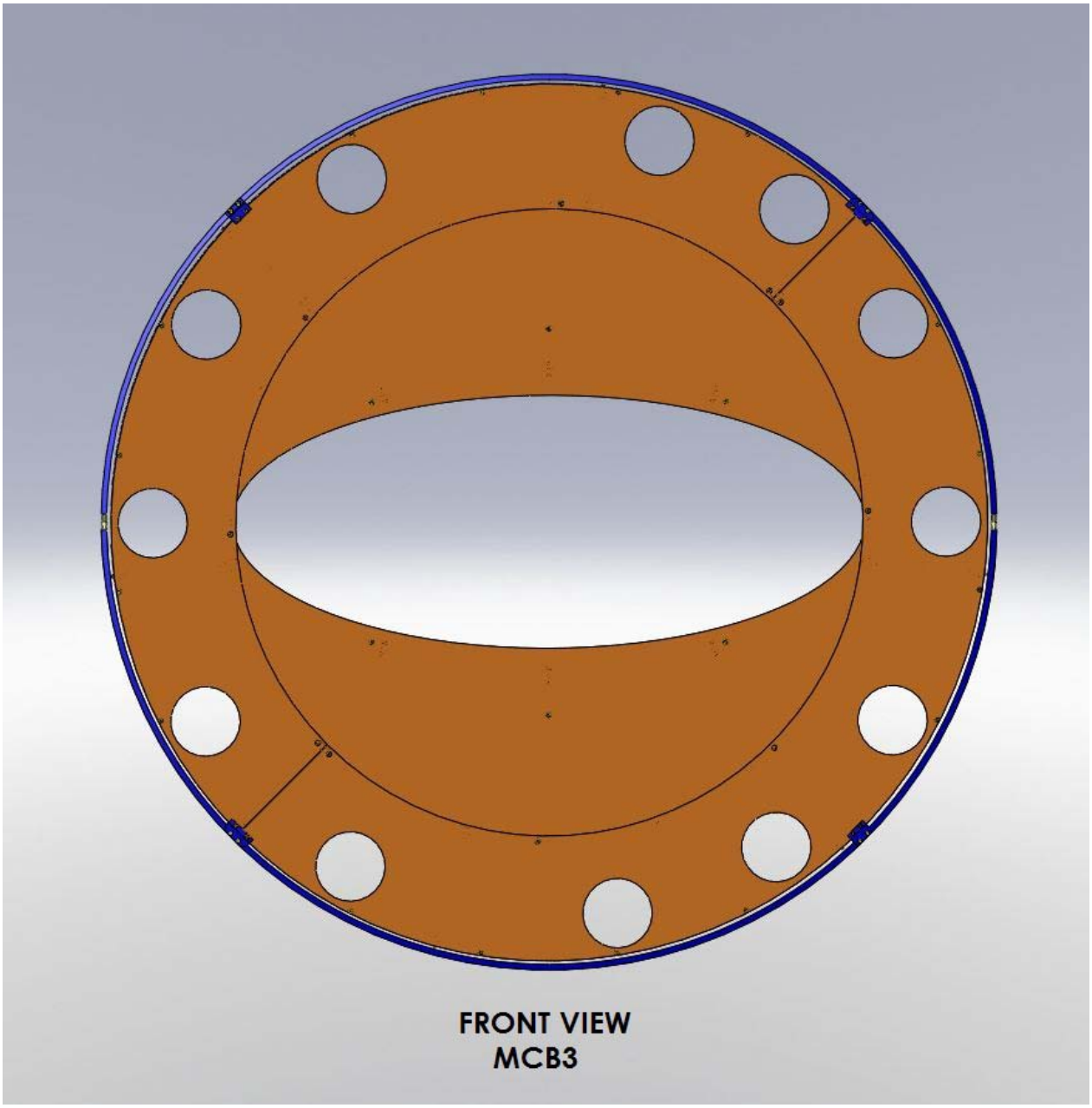

Figure 15: Front View of MCB3 Mode Cleaner Tube Baffle

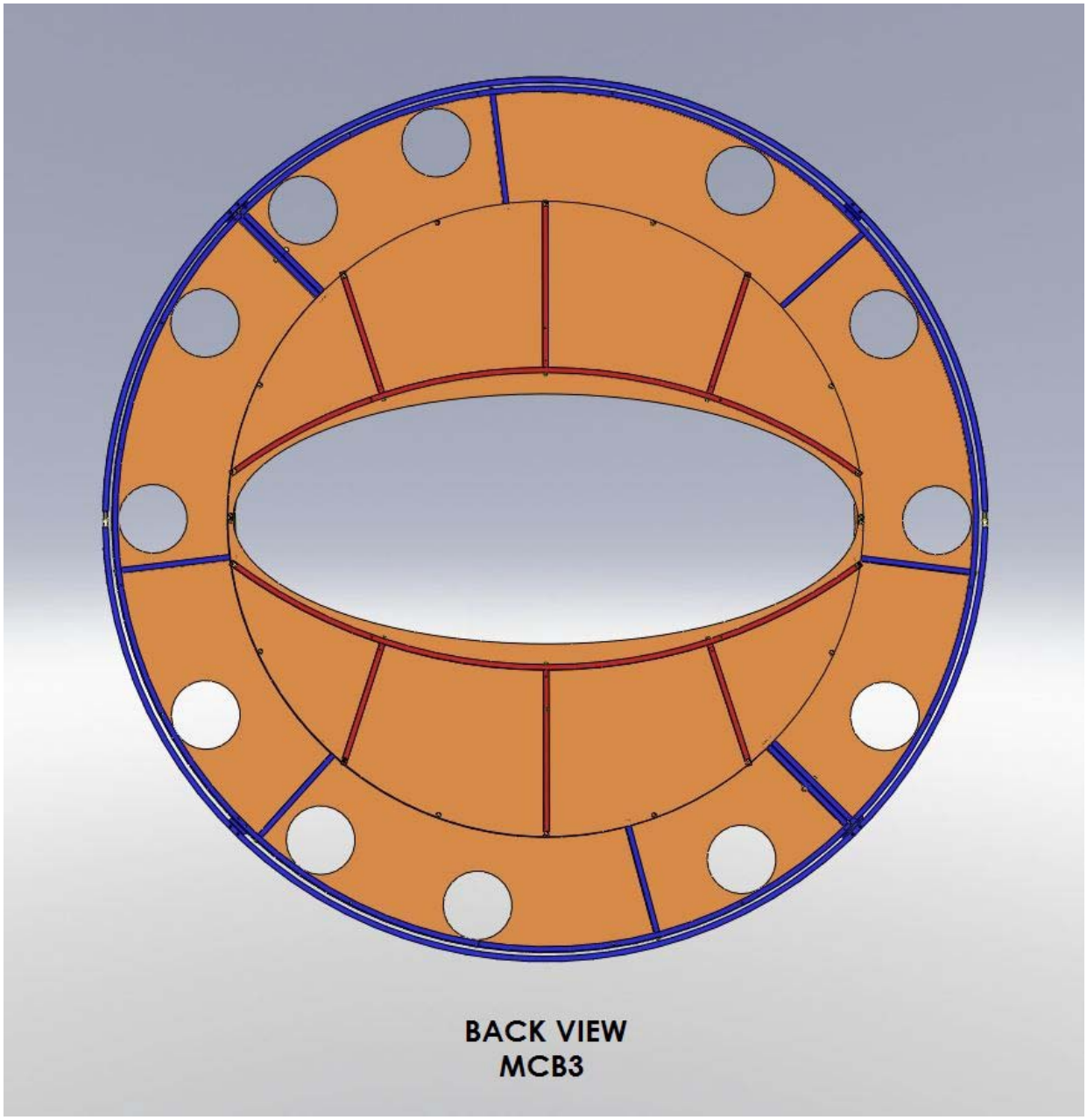

Figure 16: Back View of MCB3 Mode Cleaner Tube Baffle

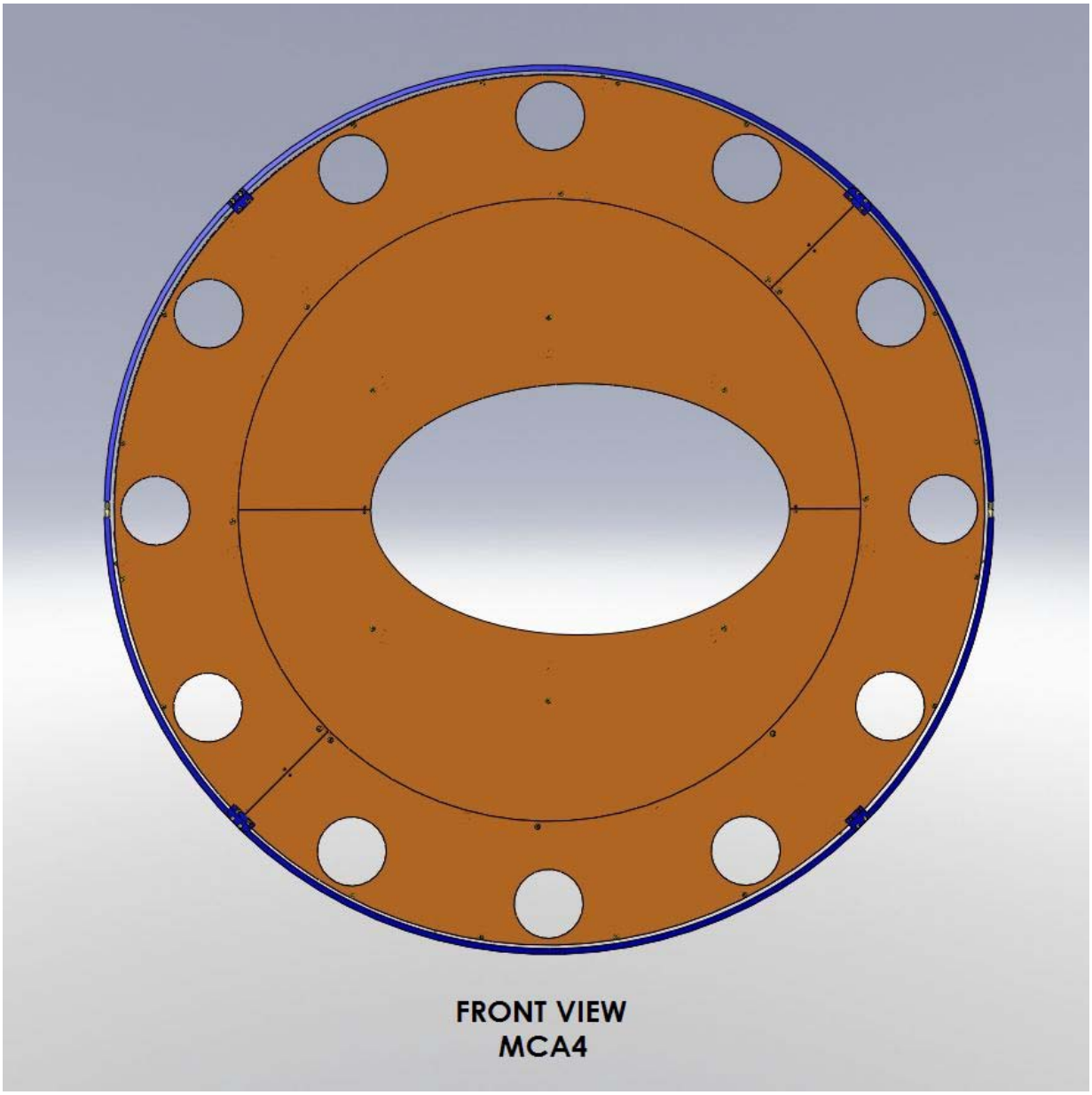

Figure 17: Front View of MCA4 Mode Cleaner Tube Baffle

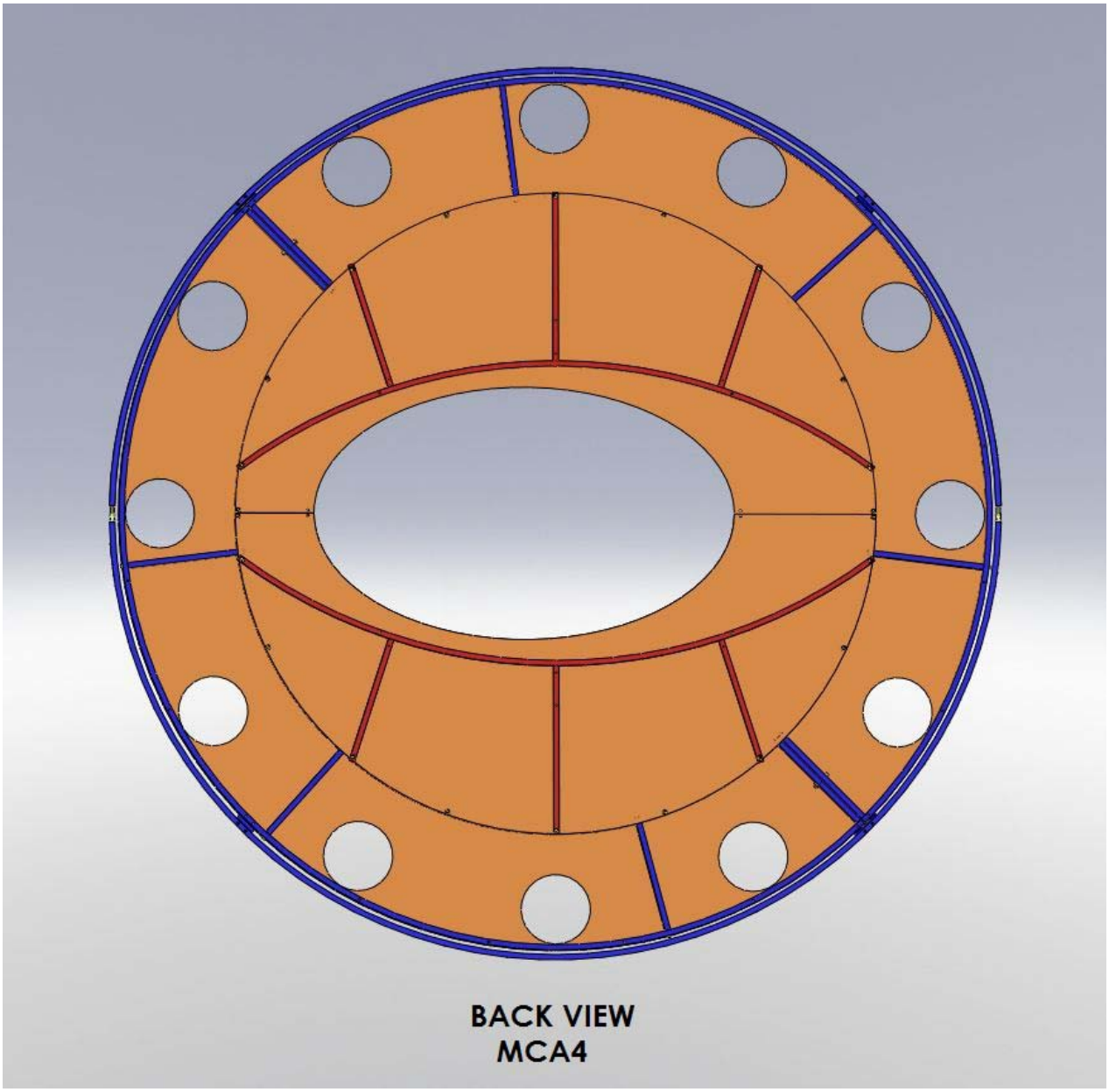

Figure 18: Back View of MCA4 Mode Cleaner Tube Baffle

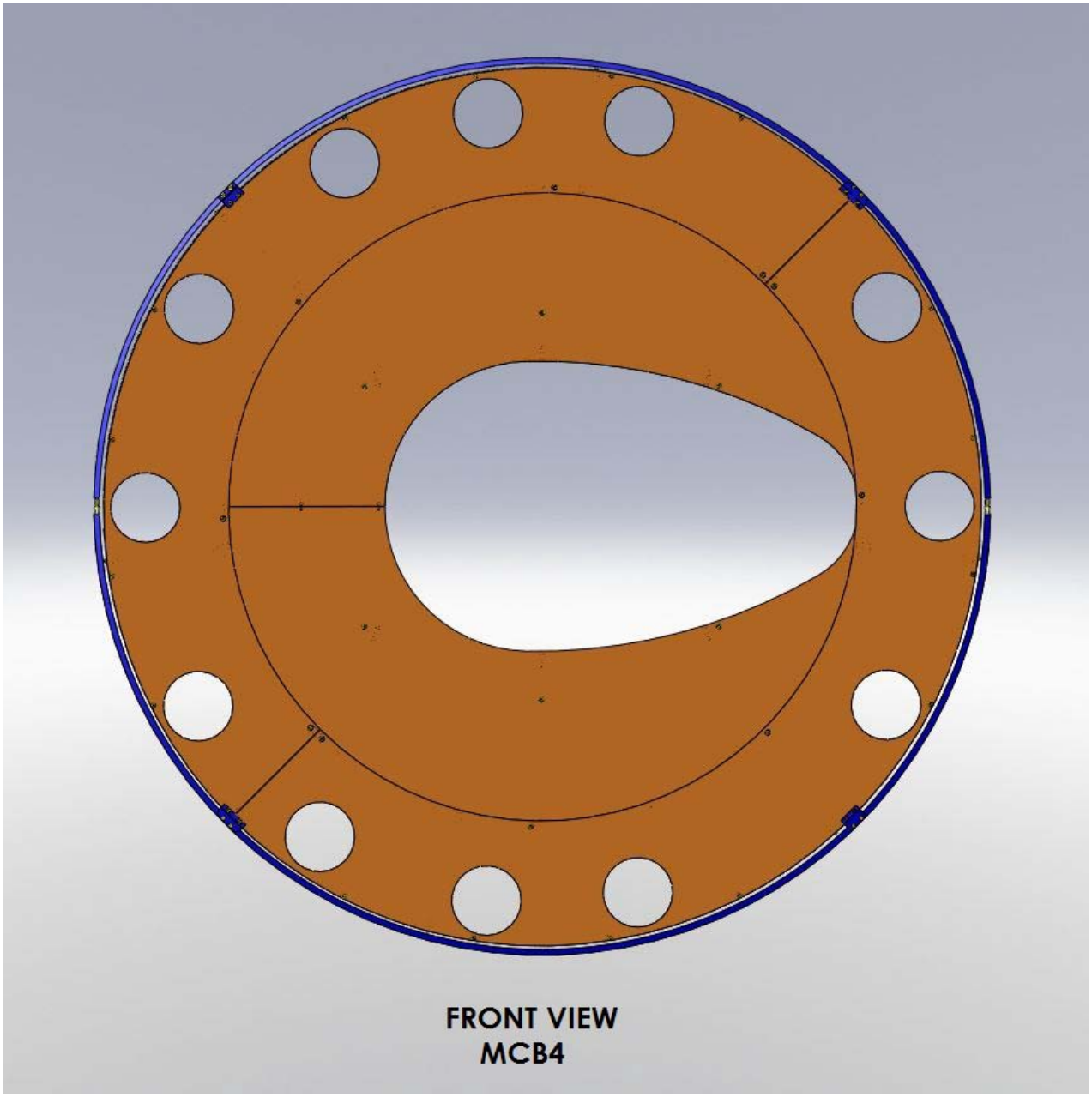

Figure 19: Front View of MCB4 Mode Cleaner Tube Baffle

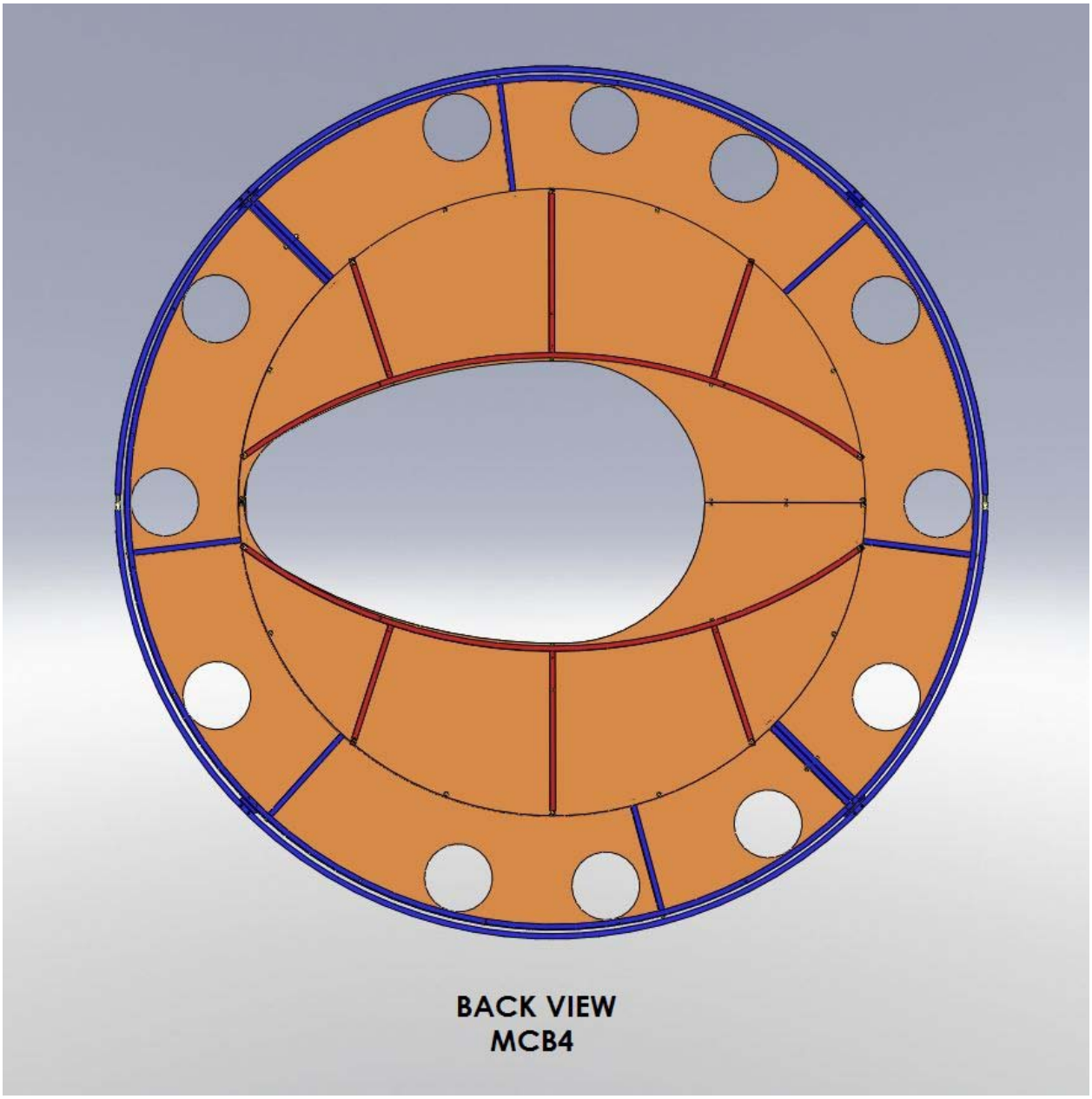

Figure 20: Back View of MCB4 Mode Cleaner Tube Baffle

2.4 Errant Beam Damage of the Mode Cleaner Tube Baffle

2.4.1 Loss of Lock of Power Recycling Cavity

If the power recycling cavity looses lock because of an errant PR2 mirror. The photons stored in the arm cavity will leak out at a rate dependent upon the reflection coefficient of the ITM mirror of the arm cavity. The errant PR2 mirror will sweep a 2 mm diameter beam around toward HAM2 or

HAM8, and the stored energy dumped from the arm cavity may hit the mode cleaner tube baffle with a damaging flux.

PSL power, W

$P_{psl} := 125$

arm cavity baffle power, W

$P_a := 840000$

length of arm cavity, m

$L_a := 4000$

reflectivity of ITM
see(T0900043)

$R_{itm} := 1 - T_{itm} = 0.986$

reflection coefficient of ITM

$r_{itm} := \sqrt{R_{itm}} = 0.993$

one transit time in arm cavity, sec

$\tau := \frac{L_a}{c} = 1.333 \times 10^{-5}$

storage time in arm cavity, sec
(ref: Fundamentals of IFO Gravity Wave detectors, Saulson, eqtn 6.22)

$t_s := \tau \cdot \frac{r_{itm}}{1 - r_{itm}} = 1.885 \times 10^{-3}$

average power during pulse, W

$P_{eave} := \frac{1}{t_s} \cdot \int_0^{t_s} P_e(t)\ t$

$P_{eave} = 1.487 \times 10^4$

resonant frequency of PR2, rad/sec
T0900435

$f_{pr2} := 1 \cdot 2 \cdot \pi = 6.2832$

length from PR2 to mode cleaner tube baffle, m

$L_b := 13.7$

arc travel of errant beam during pulse, m

$\Delta l := 2 \cdot L_b \cdot f_{pr2} \cdot t_s = 0.324$

In the following calculation, we will show that any sort of coating or oxide layer on the mode cleaner tube baffle will experience an excessively high temperature gradient across the layer and cause the layer to be damaged.

absorptivity of oxidized steel

$a_{ox} := 0.9$

absorptivity of bare aluminum $a_{al} := 0.1$

absorptivity of porcelainized steel $a_{porc} := 0.98$

thermal conductivity of iron oxide, W/m-K (estimated) $k_{sso} := 1$

thermal conductivity of aluminum, W/m-K $k_{al} := 250$

thermal conductivity of porcelain, W/m-K $k_{p} := 1$

thickness of SS oxide layer, m $tk_{sso} := 5 \cdot 10^{-6} = 5 \times 10^{-6}$

thickness of aluminum baffle, m $tk_{al} := 0.125 \cdot .0254 = 3.175 \times 10^{-3}$

thickness of porcelain layer, m $tk_{porc} := 0.005 \cdot .0254 = 1.27 \times 10^{-4}$

Then, the temperature differentials due to conduction through the iron oxide film or through the porcelain layer are given by

temperature differential across iron oxide film, deg C

$$\Delta T_{ksso} := \frac{a_{os} \cdot P_{eave} \cdot d}{k_{sso} \cdot \left(2 \cdot tk_{sso} \cdot \Delta l\right)}$$

$$\Delta T_{ksso} = 8.248 \times 10^{6}$$

temperature differential across porcelain thickness, deg C

$$\Delta T_{kp} := \frac{a_{porc} \cdot P_{eave}}{\left[k_{p} \cdot (d \cdot \Delta l)\right]} \cdot l_{dporc}$$

$$\Delta T_{kp} = 568.351$$

Clearly because of the large temperature rise, the oxide and porcelain layers will be damaged during the errant beam pulse.

However, if the baffle is made of pure aluminum the small temperature differential will not cause damage.

temperature differential across aluminum thickness, deg C

$$\Delta T_{kal} := \frac{a_{al} \cdot P_{eave}}{\left[k_{al} \cdot (d \cdot \Delta l)\right]} \cdot l_{dal}$$

$$\Delta T_{kal} = 3.646$$

2.4.2 Loss of Lock of Input Mode Cleaner Cavity

Similarly, if the input mode cleaner cavity looses lock because the MC1, MC2, or MC3 mirror moves inadvertently, the stored beam energy may be directed toward the mode cleaner tube baffle and cause damage.

The photons stored in the IMC cavity will leak out at a rate dependent upon the reflection coefficient of the IMC cavity.

IMC cavity power, W

$$P_{imc} := 23000$$

length of IMC cavity, m

$$L_{imc} := 16$$

reflectivity of IMC (see T060269)

$$R_{imc} := 1 - T_{imc} = 0.994$$

reflection coefficient of ITM

$$r_{imc} := \sqrt{R_{imc}} = 0.997$$

The storage time in the input mode cleaner cavity is considerable shorter than that of the arm cavity, because of the shorter length of the mode cleaner cavity.

one transit time in IMC cavity, sec

$$\tau := \frac{L_{imc}}{c} = 5.333 \times 10^{-8}$$

storage time in IMC cavity, sec (ref: Fundamentals of IFO Grav Wave detectors, Saulson, eqtn 6.22)

$$t_s := \tau \cdot \frac{r_{imc}}{1 - r_{imc}} = 1.77 \times 10^{-5}$$

The average power during the dump of the mode cleaner stored energy is correspondingly smaller.

average power during pulse, W

$$P_{eave} := \frac{1}{t_s} \cdot \int_0^{t_s} P_e(t) \, t$$

$$P_{eave} = 87.233$$

and, the temperature rise during the pulse will not damage the baffle, no matter from what material it is made.

2.4.3 Continuous PSL Errant Beam Power

The temperature rise due to a continuous PSL beam transmitting through the PRM mirror that is re-directed by the PR2 to a spot on the aluminum baffle is negligible.

2.5 Errant Beam Damage of the Mode Cleaner Tube Baffle

2.6 Mechanical Interfaces

The Mode Cleaner Baffles are located at both ends of the mode cleaner tubes in the power recycling and signal recycling cavities. They are attached to an outer support ring, which is compressed against the inside surface of the mode cleaner tubes.

2.7 Optical Interfaces

2.7.1 Main IFO Beams

The power recycling cavity beams and the signal recycling cavity beams pass through clearance holes in the mode cleaner baffle plates. See T1100165. The clearance holes in MCA1 for H1 and L1, and in MCA3 for H2 are larger than the 1ppm radius of the PR3 and PRM main IFO beams, as shown in the following table—the beam sizes were taken from T0900043-v10.

All the other baffle plates have a single large opening that provides adequate clearance for the IFO recycling beams.

Table 1: Mode Cleaner Tube Baffle Clearance Hole Radius, mm

IFO	BEAM	BEAM RADIUS, mm	BEAM RADIUS 1PPM, mm	MCA 1	MCA 2	MCA 3	MCA 4	MCB 1	MCB 2	MCB 3	MCB 4
H1	PR3	54	141.9	165	clear	clear	clear	clear	clear	clear	clear
H1	PR2	6.2	16.3	clear	clear	clear	clear	clear	clear	clear	clear
H1	PRM	2.2	5.8	97.8	clear	clear	clear	clear	clear	clear	clear
H1	SR3	54	141.9	clear	clear	clear	clear	clear	clear	clear	clear
H1	SR2	8.2	21.5	clear	clear	clear	clear	clear	clear	clear	clear
H1	SRM	2.1	5.5	clear	clear	clear	clear	clear	clear	clear	clear
L1	PR3	54	141.9	165	clear	clear	clear	clear	clear	clear	clear
L1	PR2	6.2	16.3	clear	clear	clear	clear	clear	clear	clear	clear
L1	PRM	2.2	5.8	97.8	clear	clear	clear	clear	clear	clear	clear
L1	SR3	54	141.9	clear	clear	clear	clear	clear	clear	clear	clear

IFO	BEAM	BEAM RADIUS, mm	BEAM RADIUS 1PPM, mm	MCA 1	MCA 2	MCA 3	MCA 4	MCB 1	MCB 2	MCB 3	MCB 4
L1	SR2	8.2	21.5	clear	clear	clear	clear	clear	clear	clear	clear
L1	SRM	2.1	5.5	clear	clear	clear	clear	clear	clear	clear	clear
H2	PR3	54.5	143.2	clear	clear	190.5	clear	clear	clear	clear	clear
H2	PR2	6.3	16.6	clear	clear	clear	clear	clear	clear	clear	clear
H2	PRM	2.1	5.5	clear	clear	97.8	clear	clear	clear	clear	clear
H2	SR3	54.2	142.4	clear	clear	clear	clear	clear	clear	clear	clear
H2	SR2	6.6	17.3	clear	clear	clear	clear	clear	clear	clear	clear
H2	SRM	2.6	6.8	clear	clear	clear	clear	clear	clear	clear	clear

The locations of the various beam holes in the baffle plates were determined by projecting 3D model beams using the following CAD files from the IO layouts and from ZEMAX layouts:

D0901920 H1 Zemax layout

D0902345 H2 Zemax Layout

D0902216 L1 Zemax layout

IO Layouts:

D0901974_ALIGO IO LHO FOLDED LAYOUT MAIN BEAM

D1100925 ALIGO IO H2 MC1, CAMERA VIEW
- D1100926 ALIGO IO H2 MC2, CAMERA VIEW
- D1100927 ALIGO IO H2 MC3, CAMERA VIEW
- D1100928 ALIGO IO H2 PRM, CAMERA VIEW
- D1100929 ALIGO IO H2 PR2, CAMERA VIEW
- D1100930 ALIGO IO H2 PR3, CAMERA VIEW

D0900919 ALIGO IO LAYOUT LLO BCS (Temp) is top assembly of:
- D1002917 ALIGO IO L1 LAYOUT PR3, OPTICAL LEVER BEAM
- D1002918 ALIGO IO L1 LAYOUT HAM2, OPTICAL LEVER BEAM
- D1002919 ALIGO IO L1 LAYOUT HAM3, OPTICAL LEVER BEAM
- D1002920 ALIGO IO L1 LAYOUT MC2, CAMERA VIEW
- D1002921 ALIGO IO L1 LAYOUT PR2, CAMERA VIEW
- D1002922 ALIGO IO L1 LAYOUT PRM, CAMERA VIEW
- D1002923 ALIGO IO L1 LAYOUT PR3, CAMERA VIEW
- D1002924 ALIGO IO L1 LAYOUT MC1, CAMERA VIEW
- D1002925 ALIGO IO L1 LAYOUT MC3, CAMERA VIEW

2.7.2 Optical Lever Beams

The H2 and H1 optical laser beams pass through the openings in the mode cleaner baffle plates that match the clear aperture of the viewports.

2.7.3 Video Camera Beams

Video camera beams pass through openings in the mode cleaner baffle plates that match the clear aperture of the viewports.

3 MANIFOLD/CRYOPUMP BAFFLE

The Manifold/cryopump Baffle is a combination of the manifold baffle and the cryopump baffle, and is located inside the manifold tube leading to the test mass near the cryopump at each end of the arm beam tube, as shown in Figure 21. The combined baffle consists of an outer cylinder, a cone, an inner cylinder, and an annular baffle plate.

The manifold baffle portion catches wide-angle scattered light from the ITM or ETM test masses, and the cryopump baffle portion obscures the interior surfaces of the nearby cryopump from the line of sight as viewed from the ITM HR or ETM HR surfaces and catches the narrow angle scattered light from the far test mass at the opposite end of the beam tube.

The baffles are suspended together from vertical blade springs by a pendulum rod, and the pitch, yaw, and vertical motions of the suspended baffle are damped with eddy current damping magnets attached to the sides of the baffle and a copper plate attached to the outer support ring. The blade springs are also mounted to the outer support ring, which is compressed against the inside surface of the manifold near the A-1 adapter.

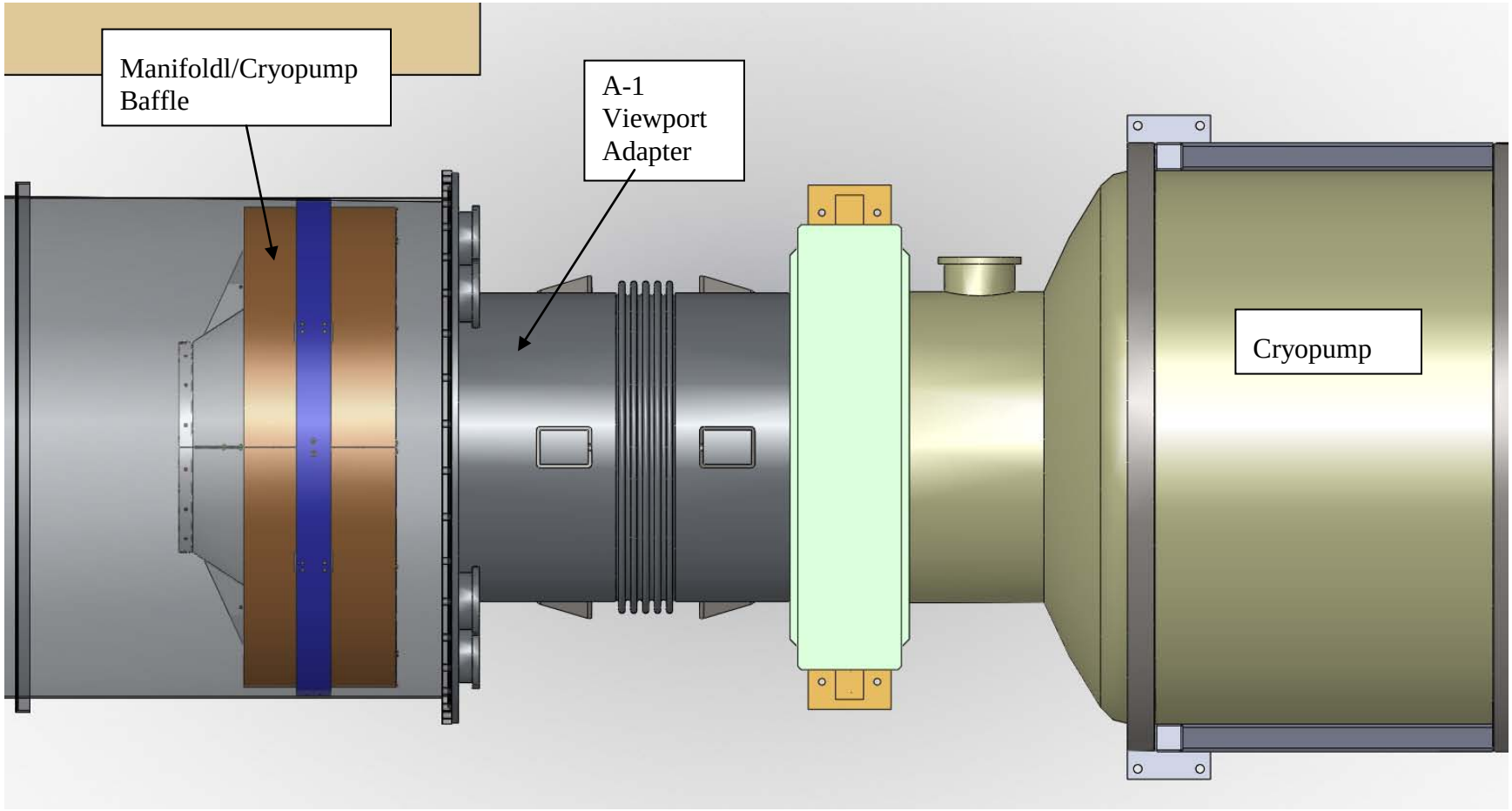

Figure 21: Manifold/Cryopump Baffle Positioned in the Manifold Tube near A-1 Viewport Adapter

A view of the manifold baffle in Figure 22, as seen from the near test mass, shows the trapping region between the outer cylinder and the outer surface of the cone that hides the corner where the manifold tube meets the flat surface of the A-1 adapter. The openings in the baffle allow the passage of optical lever beams, video beams, and photon calibrator beams.

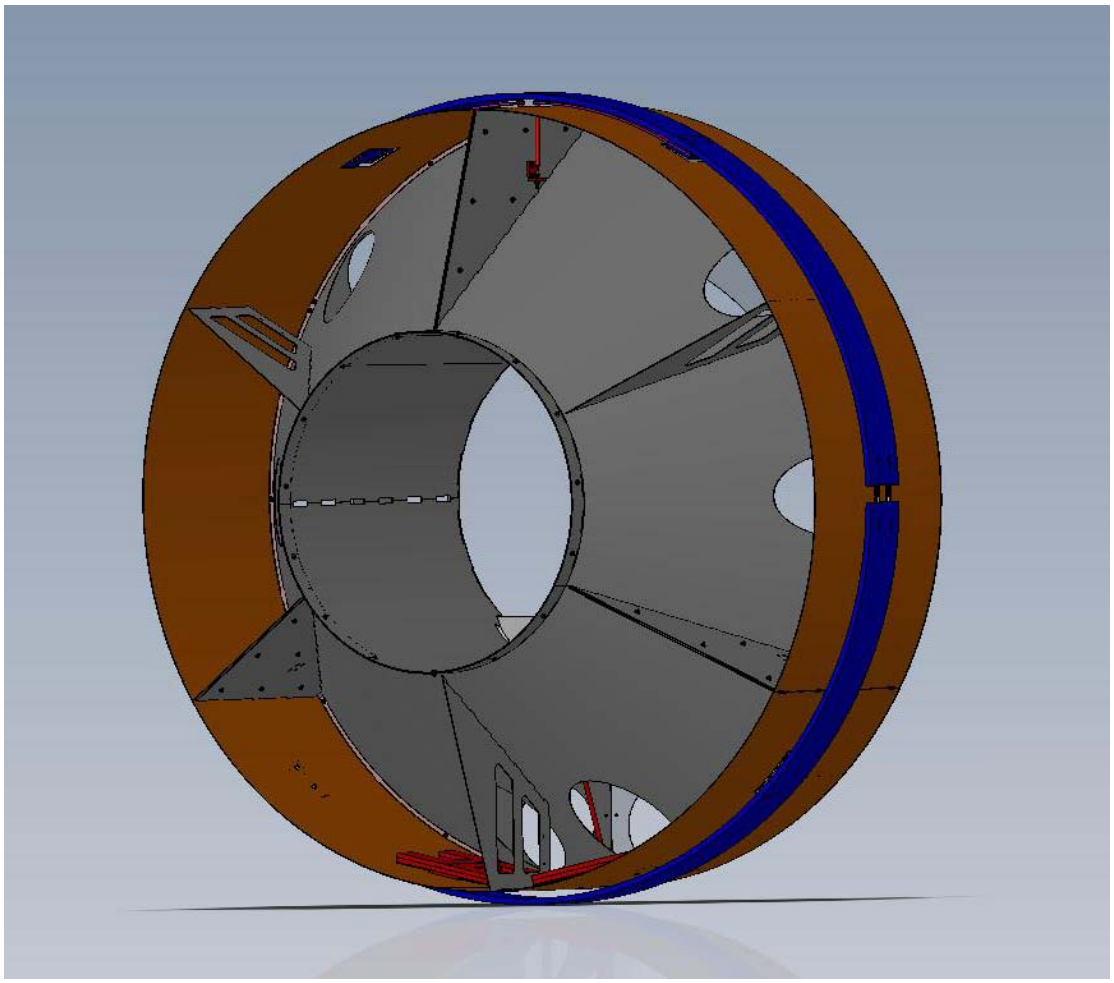

Figure 22: Manifold/Cryopump Baffle as Seen from the Near Test Mass

The side of the baffle that faces toward the cryopump and the arm beam tube, as seen in Figure 23, has an annular trapping region comprised of the inner cylinder, the inner surface of the cone, and the back of the face plate.

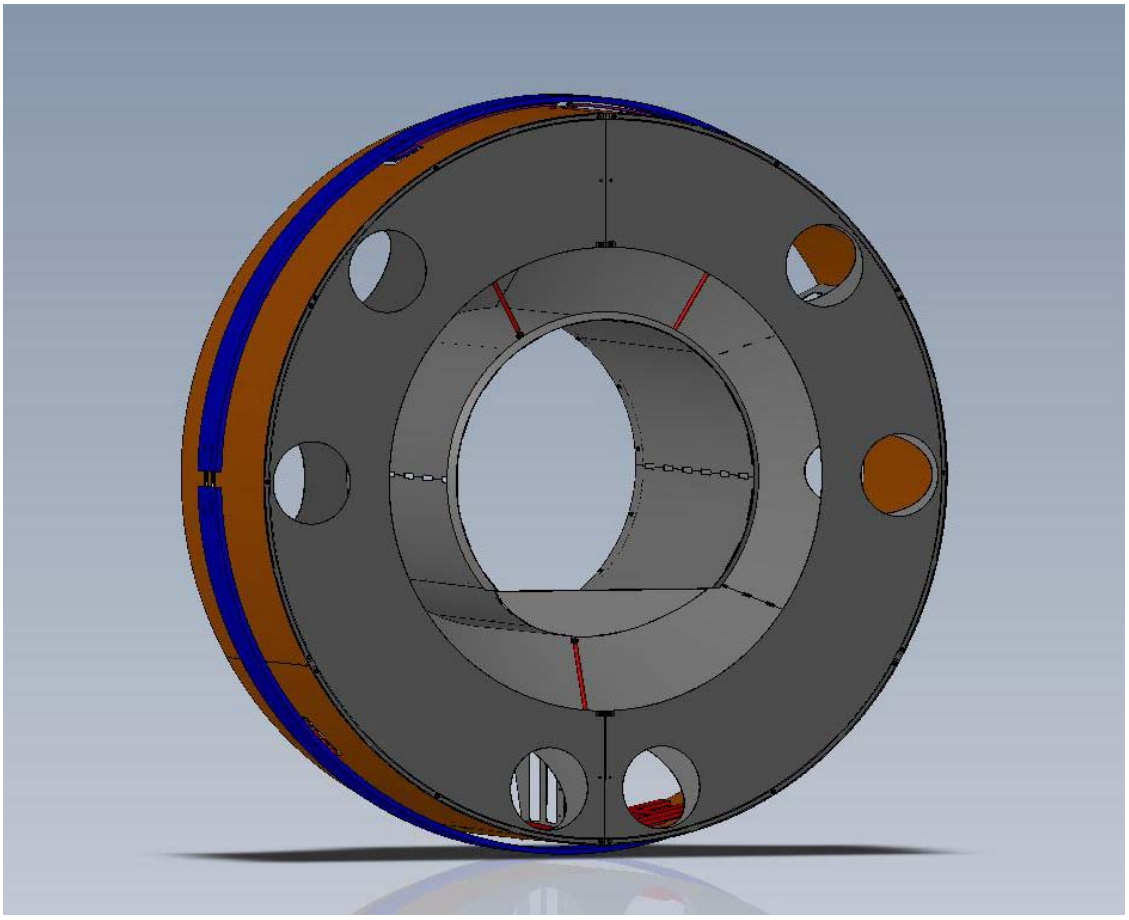

Figure 23: Manifold/Cryopump Baffle as Seen from the Cryopump and the Arm Beam Tube Direction

A photograph of the actual first article Manifold/Cryopump Baffle (without the face plate) suspended within the balancing/installation fixture is shown in Figure 24.

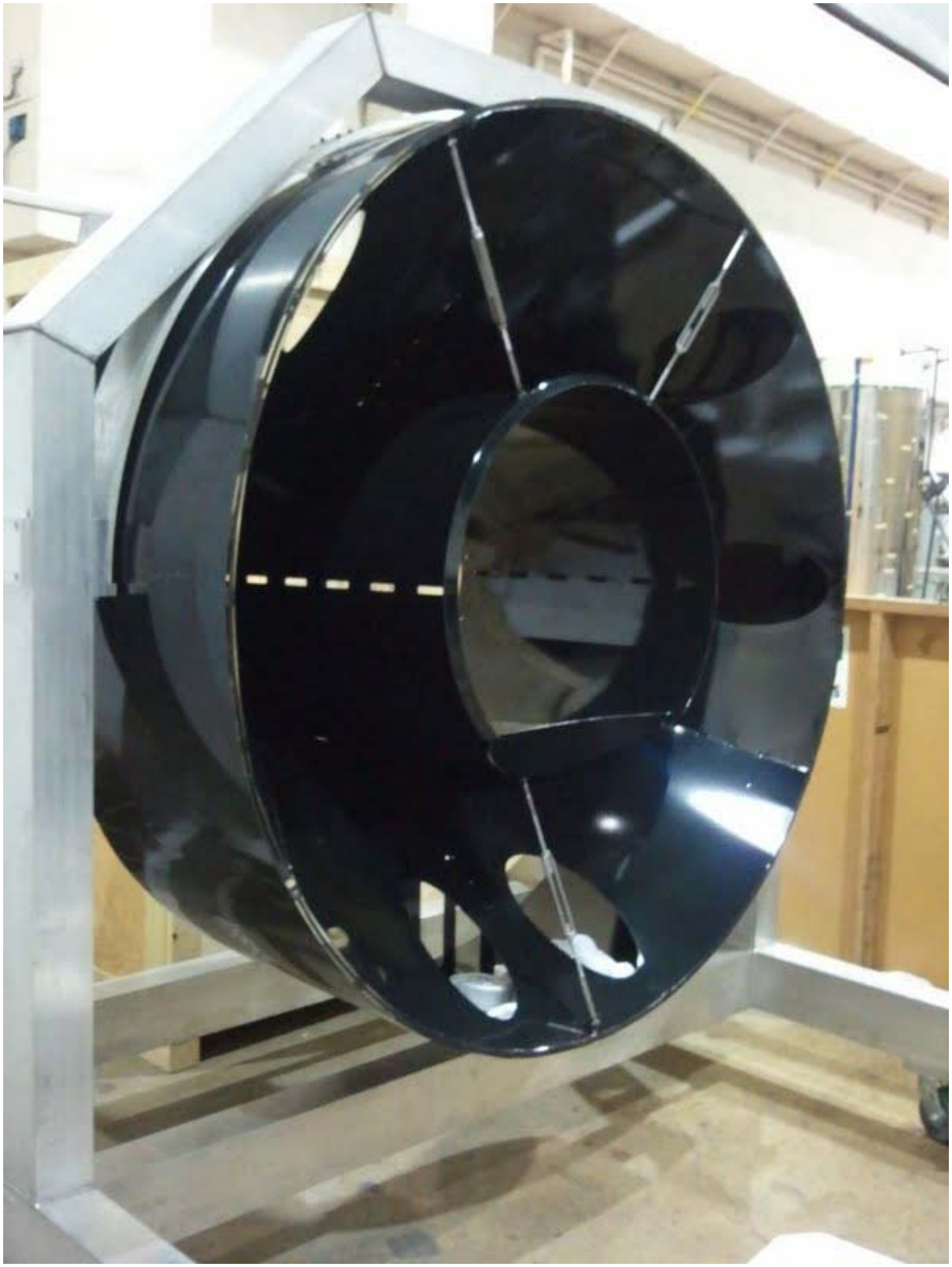

Figure 24: 1st Article Manifold/Cryopump Baffle Suspended from the Balancing/Installation Fixture

3.1 Manifold/Cryopump Baffle Characteristics

Table 2: Manifold/Cryopump Baffle Characteristics

Parameter	**Value**
Location	Corner Station-- x arm, y arm End Station-- x arm, y arm
Suspension	Vertical blade springs, 2-wire pendulum, eddy-current damping
Inside aperture diameter	769 mm
Outer diameter	1500mm
Material	Porcelainized steel
BRDF	<0.05 sr^-1
Weight	320 lbs

3.2 Manifold/Cryopump Baffle Suspension

A detailed view of the suspension structure in Figure 25 shows the two tensioned blade springs mounted to the outer support ring, with the two attachment rods that support the baffle structure. The baffle floats freely within the manifold tube.

The eddy-current damping mechanism, shown in Figure 26, consists of a copper plate mounted to the outer support ring and magnets on a steel plate mounted to the support ribs of the suspended baffle.

Also shown are balance weights located along the bottom edge of the suspended outer cylinder.

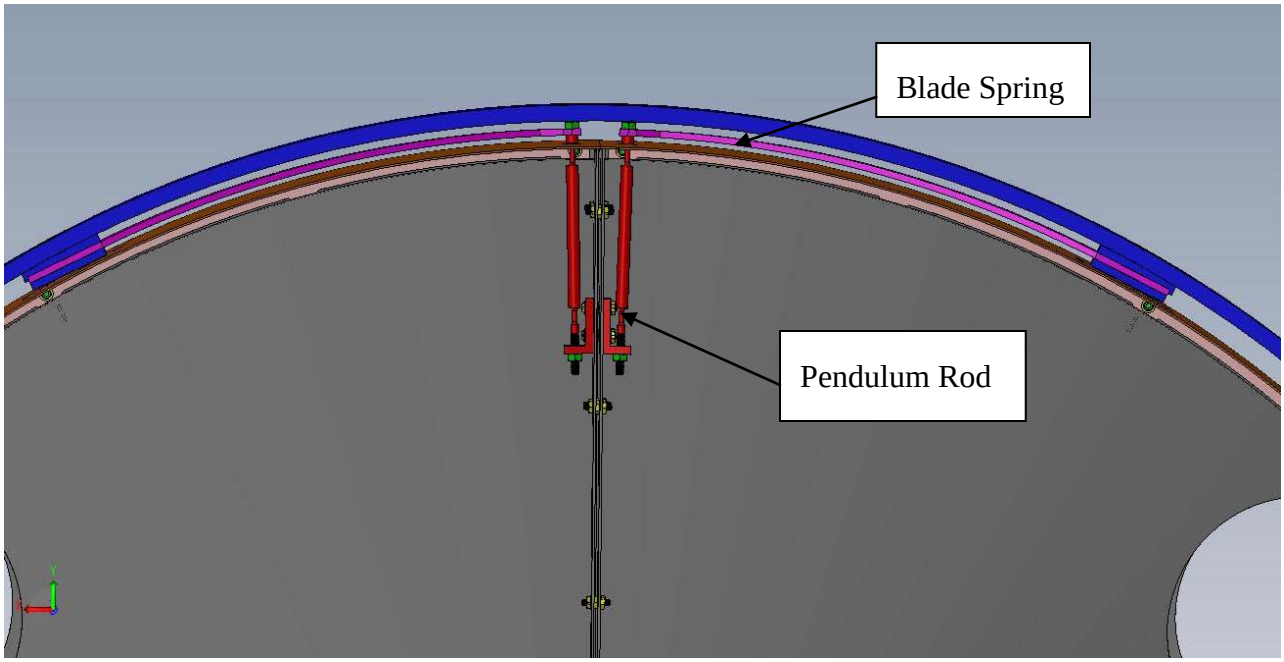

Figure 25: Close up of Blade Spring and 2-Wire Pendulum Suspension Mechanism

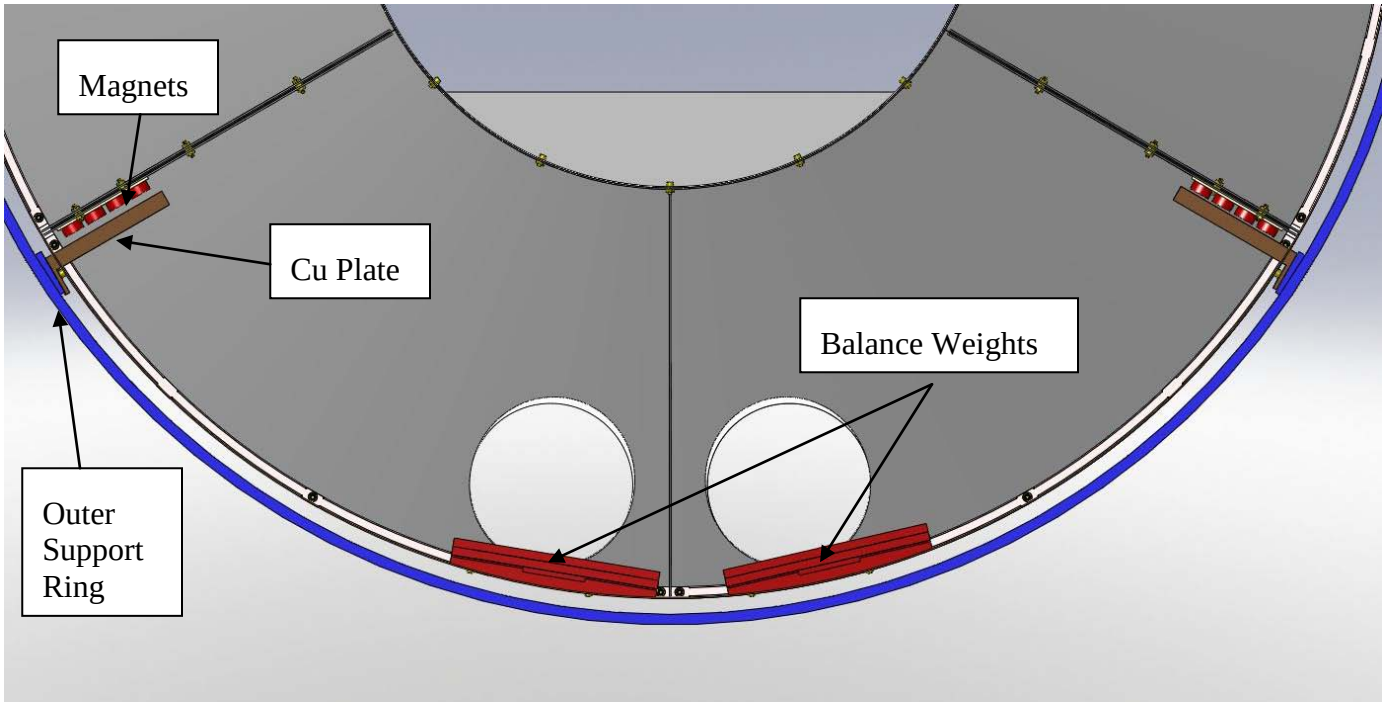

Figure 26: Eddy-current Damping Mechanism

3.2.1 Motion Transfer Function

The vertical and axial motion transfer functions were measured with the Manifold/Cryopump Baffle suspended in the balancing fixture, and are shown in Figure 27 and Figure 28.

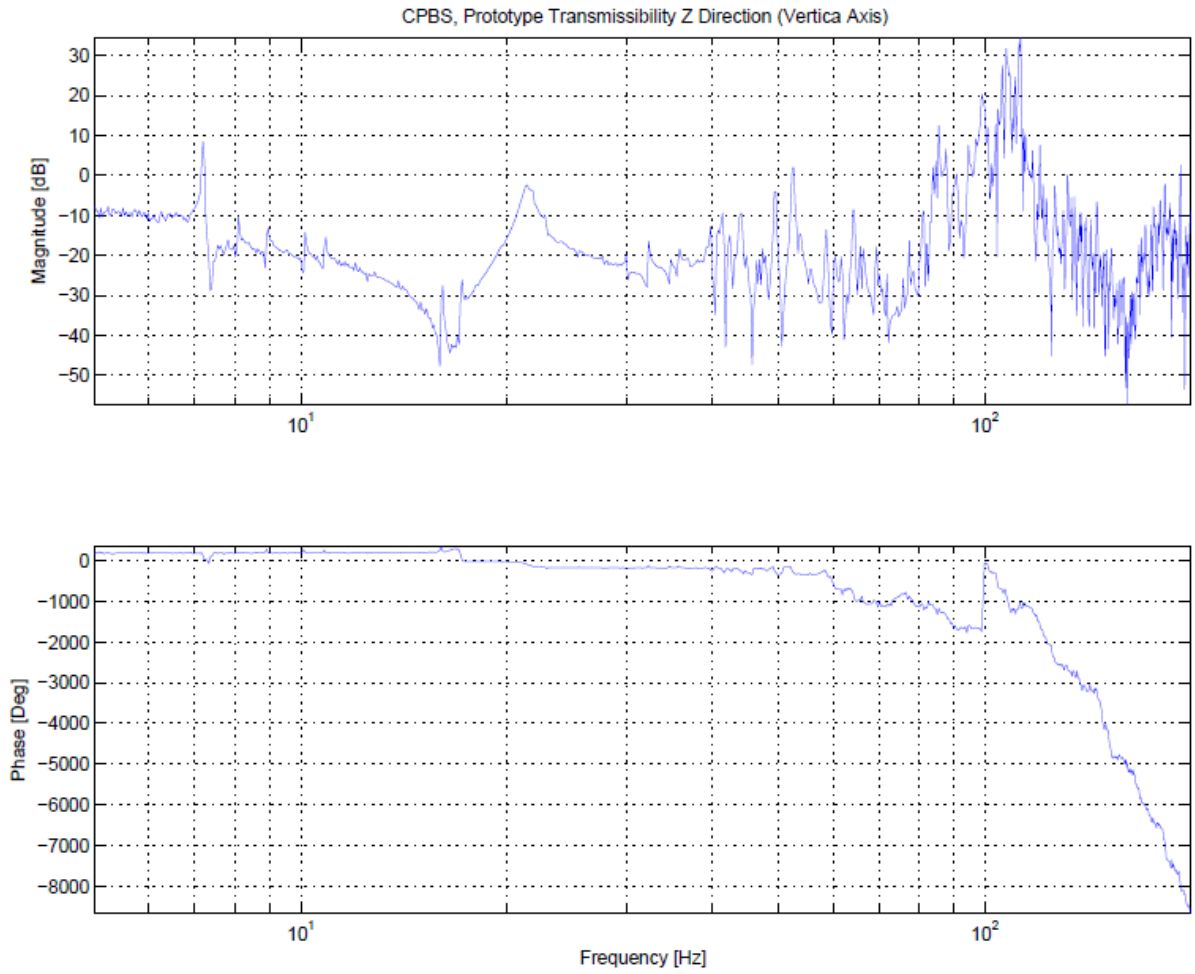

Figure 27: Vertical Transfer Function of Suspended Manifold/Cryopump Baffle

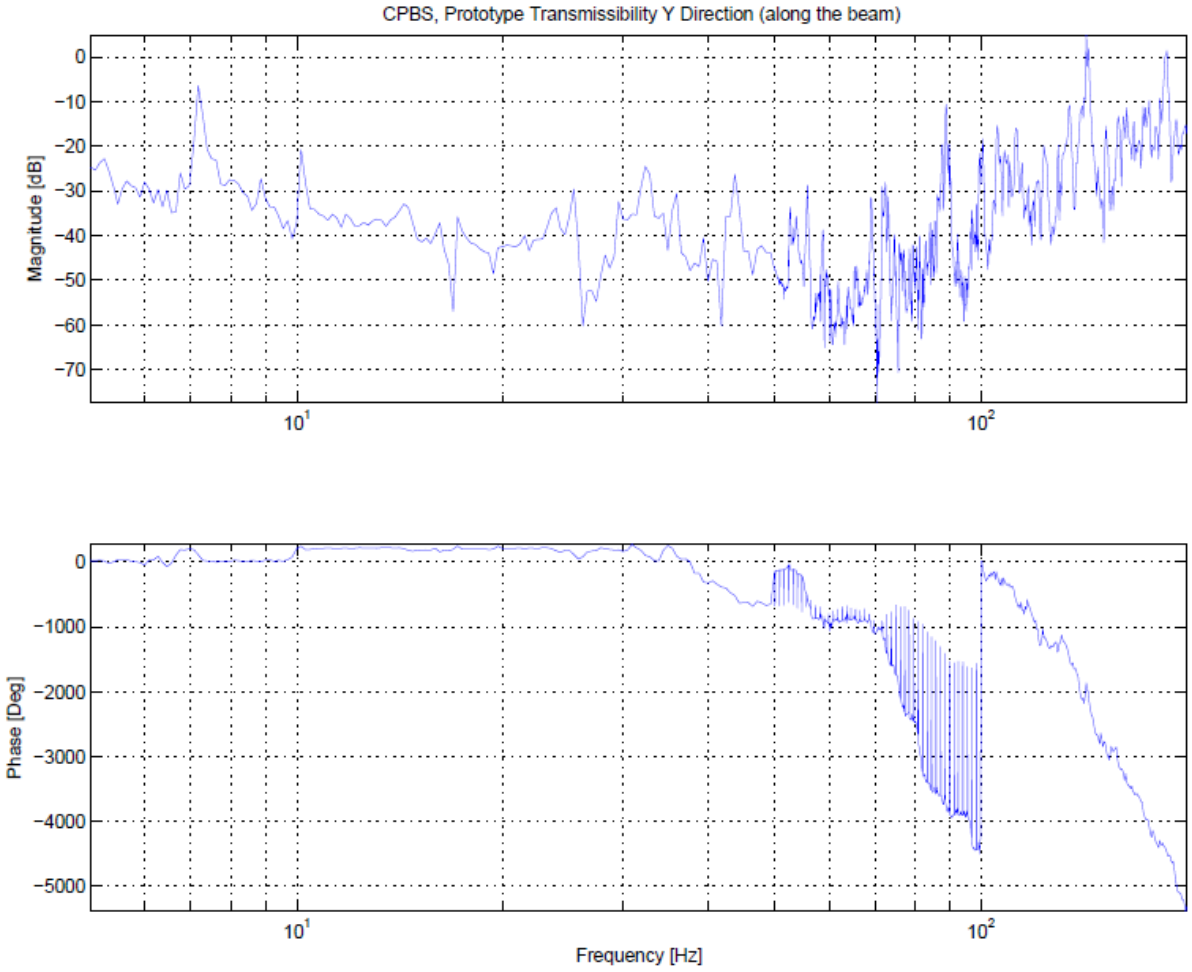

Figure 28: Axial Transfer Function of Suspended Manifold/Cryopump Baffle

3.2.2 Cryopump Baffle Surface BRDF

The Cryopump Baffle is constructed of porcelainized steel with the first surface inclined at an incidence angle 57 deg. The measured BRDF is < 0.05 sr^{-1}. See T1100056 Arm Cavity Baffle Edge Scatter.

3.2.3 Cryopump Baffle Scatter

The scattered power from the test mass at the opposite end of the beam tube into the annular area between the opening in the Cryopump Baffle and the inside diameter of the beam tube baffles will hit the Cryopump Baffle and cause scattered light back into the IFO mode.

The power hitting the Cryopump Baffle is calculated below.

$$P_{cp} := P_a \cdot \int_{\theta_{cp}}^{\theta_{bt}} 2 \cdot \pi \cdot \theta \cdot BRDF_1(\theta)\, d\theta$$

The iLIGO pathfinder COC CSIRO, surface 2, S/N 2 was used to estimate the BRDF.

$$BRDF_1(\theta) := \frac{2755.12}{\left(1 + 8.50787 \cdot 10^{8} \cdot \theta^{2}\right)^{1.23597}}$$

Where θ_{cp} is	9.612 E-5 rad
θ_{bt} is	1.327 E-4 rad
and, P_a is the arm power	8.339 E5 W
	P_{cp} = 2.8 W

The light power scattered into the IFO mode solid angle from the four Cryopump Baffles is given by

$$P_{cps} := \sqrt{4} \cdot P_{cp} \cdot BRDF_{cp} \cdot \frac{\pi \cdot w_{ifo}^{2}}{L^{2}} \cdot BRDF_1\left(30 \cdot 10^{-6}\right) \cdot \Delta_{ifo}$$

where the appropriate scattered light noise transfer function, TF_{itmhr}, is taken from T060073-00 Transfer Functions of Injected Noise

The displacement noise (m/rt Hz) is proportional to the seismic manifold tube motion, but is reduced by the Manifold/Cryopump Baffle suspension transmissibility, cpatten.

$$DN_{cpbaf} := TF_{itmhr} \cdot \left(\frac{P_{cps}}{P_{psl}}\right)^{0.5} \cdot x_{beamtube} \cdot 2 \cdot k \cdot cpatten$$

The apparent displacement noise is shown in Figure 29. It meets the requirement.

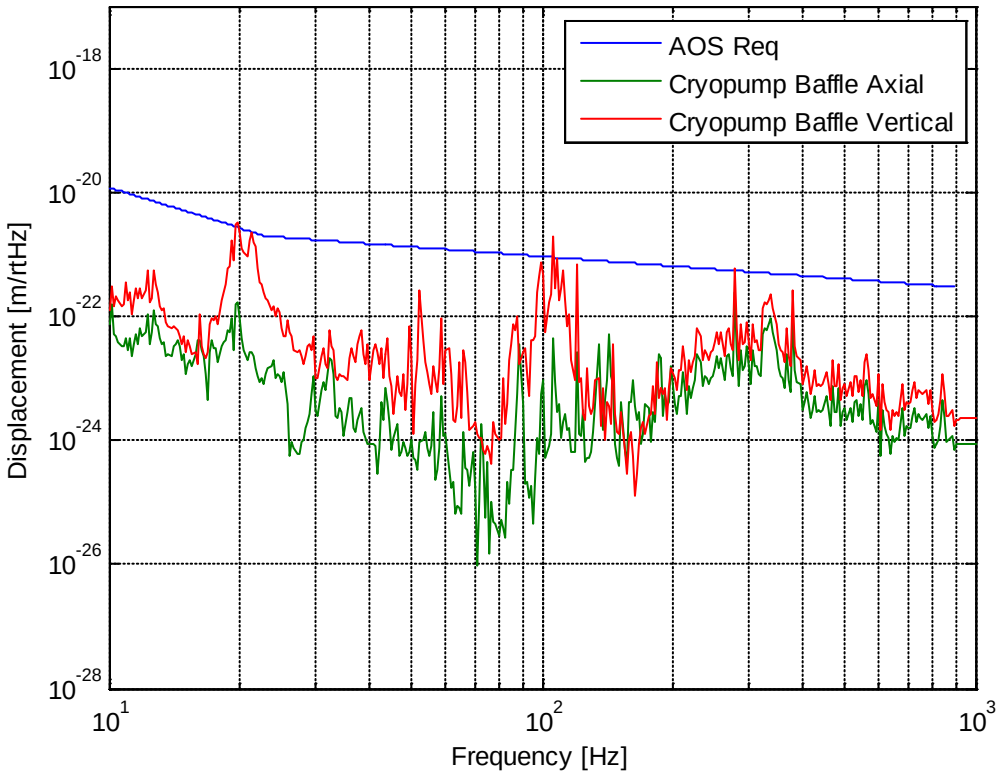

Figure 29: Cryopump Baffle Scattered Light Displacement Noise

3.3 Optical Interface

A sketch of the beam locations within the baffle opening is shown in Figure 30.

The 769 mm clear aperture diameter of the Manifold/Cryopump Baffle allows the H1 and H2 IFO arm cavity beams—< 327 mm diameter at the 1 ppm diameter—to pass through without vignetting.

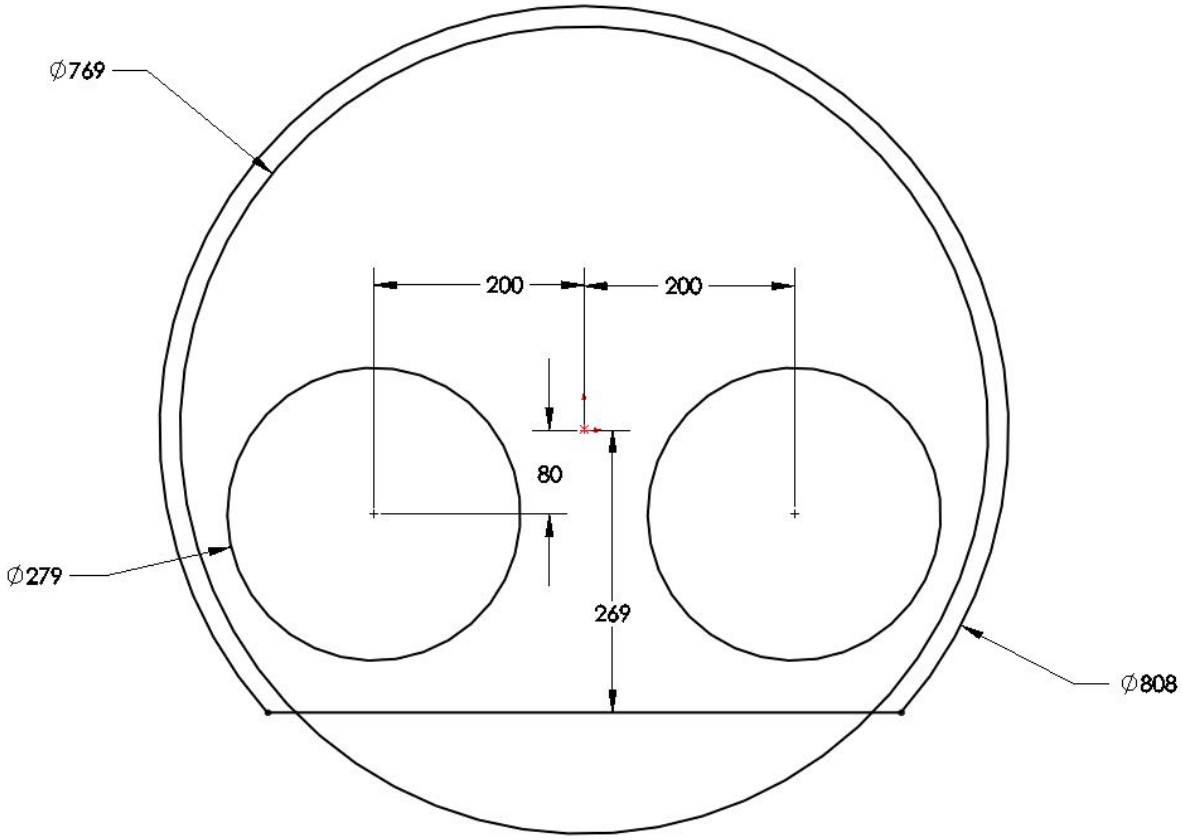

Figure 30: Clearance of Arm Cavity Beams through ITM Manifold/Cryopump Baffle

The main IFO beam is largest at the ETM baffle. The fractional arm cavity beam loss through the ETM Manifold/Cryopump baffle opening is negligible, as shown in the calculation below.

beam offset x, mm	$x_0 := -200$
beam offset y, mm	$y_0 := -80$
error offset x, mm	$\delta := 0$
cryopump radius, mm	$R := 384.5$
height of bottom ledge, mm	$h := 269$

beam radius at ITM mirror, mm $w_{ITM} = 53.109$

beam radius at ETM mirror, mm $w_{ETM} = 62.094$

beam radius ETM @ 1ppm power, mm $r_{etm1ppm} := w_{ETM} \cdot \sqrt{\frac{6}{2} \cdot \ln(10)}$

$r_{etm1ppm} = 163.199$

Intensity distribution function ETM, W/mm^2 $I(x, y, x_0, y_0, \delta) := \frac{2}{\pi \cdot w_{ETM}^2} \cdot e^{\frac{-2 \cdot \left[(x - x_0 + \delta)^2 + (y - y_0)^2 \right]}{w_{ETM}^2}}$

total power through cryopump baffle, W $P_{cryo}(\delta) := \int_{-R}^{R} \int_{-h}^{\sqrt{R^2 - x^2}} I(x, y, x_0, y_0, \delta) \, dy \, dx$

fractional power hitting the cryopump baffle $P_{hcryo}(\delta) := 1 - P_{cryo}(\delta)$

$P_{hcryo}(\delta) = 1.894 \times 10^{-9}$

The manifold/cryopump baffle is insensitive to centering errors up to tens of millimeters, as shown in Figure 31.

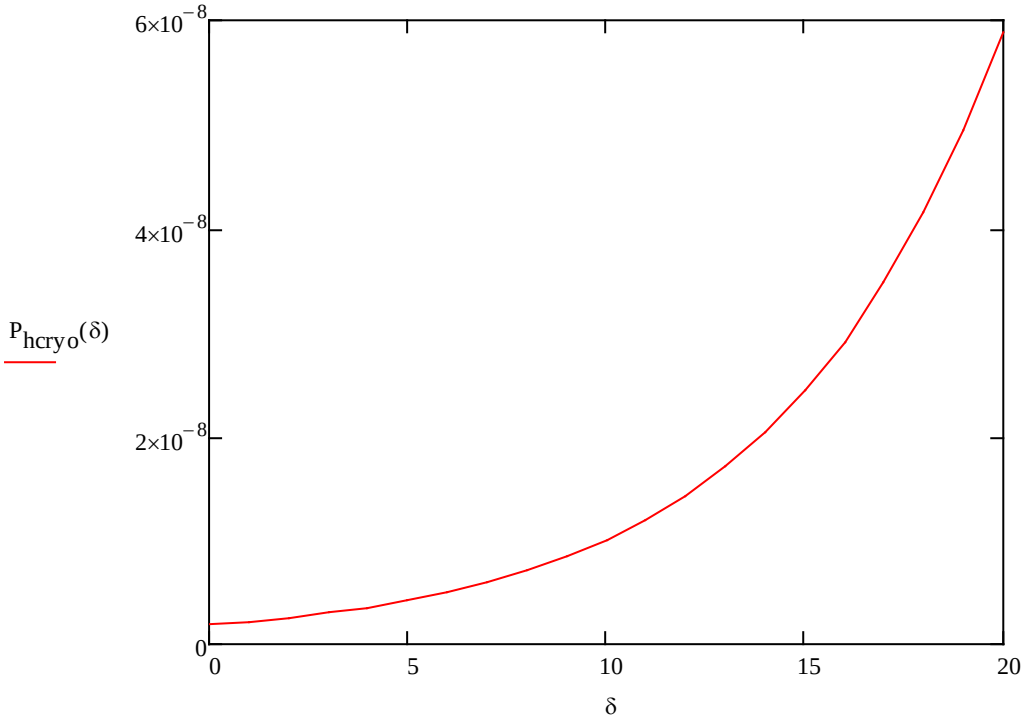

Figure 31: Manifold/cryopump Baffle Fractional Power Absorption vs Horizontal De-centering Error

4 INTERFACE CONTROL DOCUMENT

The mechanical and optical interfaces of the Manifold/cryopump Baffle and the Mode Cleaner Tube Baffles are described in E1100583 SLC Manifold/Cryopump Baffle Interface Control Document.

.